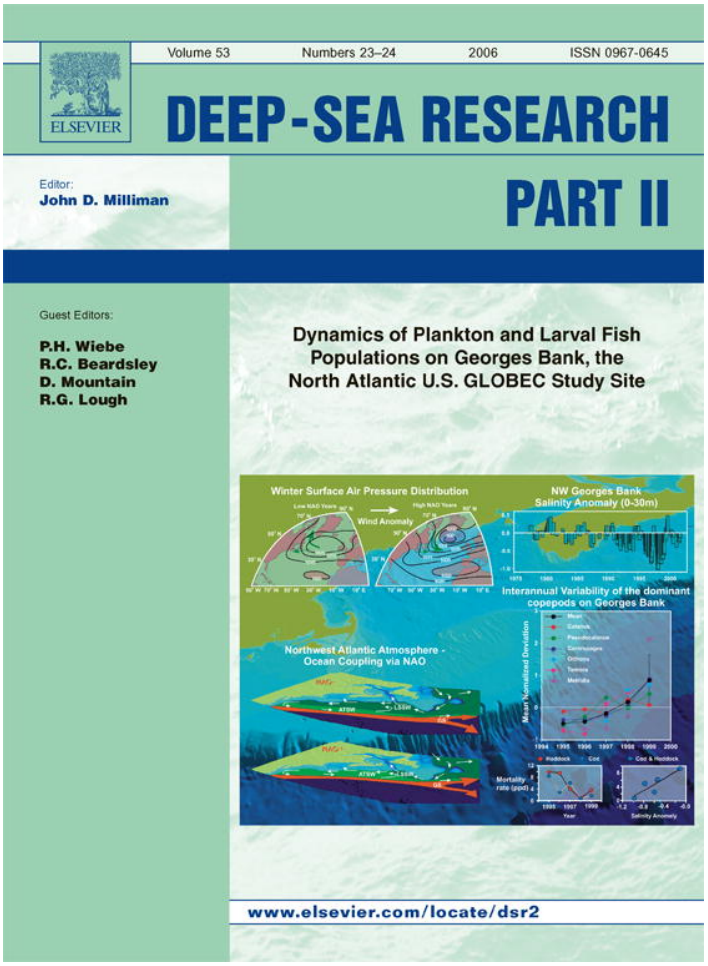

Available online at www.sciencedirect.com
ScienceDirect
Deep-Sea Research II 53 (2006) 2684–2707
DEEP-SEA RESEARCH PART II
www.elsevier.com/locate/dsr2

The impact of Scotian Shelf Water "cross-over" on the plankton dynamics on Georges Bank: A 3-D experiment for the 1999 spring bloom

Rubao Ji[a,*], Changsheng Chen[b], Peter J.S. Franks[c], David W. Townsend[d], Edward G. Durbin[e], Robert C. Beardsley[f], R. Gregory Lough[g], Robert W. Houghton[h]

[a]*Department of Biology, Woods Hole Oceanographic Institution, MS# 33, Redfield 1-32, Woods Hole, MA 02543, USA*
[b]*The School for Marine Science and Technology, University of Massachusetts Dartmouth, New Bedford, MA 02744, USA*
[c]*Integrative Oceanography Division, Scripps Institution of Oceanography, University of California, San Diego, La Jolla, CA 92093-0218, USA*
[d]*School of Marine Sciences, University of Maine, 5741 Libby Hall, Orono, Maine 04469, USA*
[e]*Graduate School of Oceanography, University of Rhode Island, South Ferry Rd, Narragansett, RI 02882, USA*
[f]*Department of Physical Oceanography, Woods Hole Oceanographic Institution, Woods Hole, MA 02543, USA*
[g]*Northeast Fisheries Science Center, National Marine Fisheries Service, NOAA, Woods Hole, MA 02543, USA*
[h]*Lamont Doherty Earth Observatory of Columbia University, Palisades, NY 10964, USA*

Accepted 28 August 2006
Available online 14 November 2006

Abstract

The 1999 March SeaWiFS images detected an intense phytoplankton bloom on the southern flank of Georges Bank (GB). The bloom covered a large portion of the southern flank between the 60 and 200 m isobaths, and later extended to and connected with an even larger patch near the Northeast Peak (NEP) and Browns Bank. A three-dimensional (3-D) model experiment was conducted to examine the cause of the bloom and the impact of Scotian Shelf Water on the spring phytoplankton bloom dynamics. The finite volume coastal ocean model (FVCOM) provided the hydrodynamic fields for Lagrangian particle trajectory, tracer and biological model experiments. Process-oriented modeling experiments showed that the formation and maintenance of the phytoplankton bloom on the southeastern flank of GB is related to the weak stratification caused by the transport of the colder but fresher Scotian Shelf Water across the Northeast Channel (NEC). With sufficient nutrients from the slope, the bloom could result from in situ growth of phytoplankton near the slope where the stabilizing salinity front is located. The model results suggest that the timing and location of the phytoplankton bloom on the southern flank of GB is sensitive to the spatial distribution of temperature and salinity on the bank, the flow fields across the NEC, and the location of the salinity front near the shelf break.

Keywords: Phytoplankton; Algal bloom; Modelling; Finite volume; Coastal Ocean model; Scotian Shelf Water

*Corresponding author. Tel.: +1 508 289 2986; fax: +1 508 457 2134.
E-mail address: rji@whoi.edu (R. Ji).

0967-0645/$ - see front matter © 2006 Elsevier Ltd. All rights reserved.
doi:10.1016/j.dsr2.2006.08.007

1. Introduction

The springtime phytoplankton bloom in the Gulf of Maine (GOM) and Georges Bank (GB) is a recurrent seasonal event that persists for weeks (Riley, 1941; O'Reilly et al., 1987; Townsend and Thomas, 2001, 2002). It usually occurs in March and April over a large area, and can be easily detected in satellite images (Thomas et al., 2003). Spring phytoplankton blooms are important in modifying the elemental composition of surface waters, providing the food source for higher trophic levels, and potentially having a long-term (months) impact on lower trophic level food web dynamics (Cloern, 1996). On GB, the timing, location and magnitude of blooms appear to be critical for the recruitment success of zooplankton populations. For example, the production rate of copepod *Calanus finmarchicus* could be limited by the lack of food (phytoplankton) on the southern flank of the bank during spring time (Campbell et al., 2001). Therefore, a detailed examination of the spatial-temporal evolution of phytoplankton blooms will improve our understanding of zooplankton population dynamics on GB, which is further related to populations in a higher trophic level, such as cod and haddock.

In a natural system, patchiness of the spring bloom is mainly controlled by (1) spatial variability in the local balance between phytoplankton production and loss and (2) spatial and temporal variations in the transports of water and phytoplankton (Lucas et al., 1999). This dynamics can be summarized by the following equation:

$$\frac{\partial C}{\partial t} = B - \nabla(VC) + \nabla(K\nabla C),$$

where $C(x, y, z, t)$ is the concentration of phytoplankton at position (x, y, z) at time t; $V(u, v, w)$ represents the advective fluid velocities in x, y, z directions; Kx, Ky, Kz are diffusivities in x, y, z directions; $\nabla = (\partial/\partial x, \partial/\partial y, \partial/\partial z)$ is the Laplacian operator; and B is the biological source and sink terms. On the left side of equation is the local rate of change of C. On the right side, the second term is advection and the third term is the diffusion term. B can vary significantly in the horizontal due to variations in water depth as well as differences in turbidity, nutrient concentrations, grazing pressures, turbulent mixing, and so on.

As suggested in 1-D and 2-D modeling studies (Ji et al., 2006), in the absence of advection the spring bloom in the deeper areas of GB could develop only when thermally induced stratification developed, usually after late April. However, observational data suggest that early spring phytoplankton blooms did occur occasionally in the deep flank areas. For instance, a significant bloom was observed on the southern flank of the bank in March 1999 (described in next section), indicating the important role of horizontal transport on the spring bloom dynamics in this area (Ji et al., 2006). Water on the northeast peak (NEP) and the southern flank could be advected from many sources, including the GOM, the southwestern Scotian Shelf, the central bank, and continental slope. Flow from the GOM onto the bank is a major pathway of water onto GB and has been described in various studies (e.g., Butman et al., 1987; Beardsley et al., 1997; Chen et al., 2001), while the flow of Scotian Shelf Water (SSW) across Northeast Channel (NEC) (referred as "cross-over" hereafter) appears to be episodic as suggested by historical data (Bigelow, 1927; Hopkins and Garfield, 1981; Flagg, 1987) and recent satellite-derived sea-surface temperature (SST) and hydrographic data (Bisagni et al., 1996). Using the low-salinity (<32 PSU) signature of SSW, Bisagni and Smith (1998) showed that "cross-over" events could be related to the passage of cyclonic eddies and recur with a 3–5 yr time scale. Water exchange between the central bank and the surrounding area is mainly controlled by wind-driven transport. Both modeling studies (e.g., Lewis et al., 2001) and drifter experiments (Naimie et al., 2001) indicate that the displacements of plankton from the central bank to the NEP and the southern flank could occur in 10 days with strong winds in a off-bank favorable direction. A final potential source is from the slope water in the form of warm-core rings (WCRs) as suggested by (Ryan et al., 1999, 2001). Interactions of WCRs with the surrounding hydrography can enhance phytoplankton biomass within the ring core and along the shelf break of GB. However, this process usually occurs during late spring (May).

Once the water flows onto the NEP and the southern flank, it follows a clockwise circulation along isobaths between about 60 and 100 m with maximum speeds of about 5–8 cm/s (Chen et al., 2001). The occurrence of blooms on the northern flank and NEP (upstream) has a significant influence on the ecosystem dynamics on the southern and southwestern flanks (downstream), since the post-bloom water from upstream is usually nutrient

depleted at the surface, and phytoplankton community structure may be altered significantly.

This study will examine the effect of SSW "cross-over" events on the spring bloom dynamics of GB, with a case study in March 1999. The major questions to be addressed are: (1) can the blooming phytoplankton patch be transported across NEC and maintain a high phytoplankton concentration? (2) what are the roles of low-salinity-induced stratification and the shelf-break front in controlling the location and movement of blooms? and (3) what is the implication of an early spring bloom for zooplankton populations on GB?

2. Observed biological features associated with a SSW "cross-over"

2.1. Views from the satellite

The 1999 March SeaWiFS data clearly show a spatially extensive bloom occurring near the NEC and Browns Bank from day 73 to 80 (Fig. 1, upper panel, Area 1). The concentration of chlorophyll *a* in this area was higher than 3.0 μg/l and reached about 8.0 μg/l in some patches. Meanwhile, an equally intense bloom was observed on the southern flank (Fig. 1, upper panel, Area 2). This patch was disconnected from the patches over the NEC and Browns Bank areas. It extended on-bank, reaching the 60 m isobath, and off-bank, reaching the 200 m isobath. Between day 81 and day 88, this relatively small patch in Area 2 seems to extend and become connected with the larger patch in Area 1 along the northeast edge of the bank (Fig. 1, middle panel). The bloom declined afterward, with only some sporadic patches remaining in the NEP and the southern edge of the bank (Fig. 1, bottom panel).

The water mass in Area 1 carried a clear signature of cold surface water temperature, as seen in Fig. 2. The intrusion of water from the Browns Bank area across the NEP occurred as early as February 16 (image labeled with "day 47" in upper left panel of Fig. 2). The signal of a cold water band "cross-over" was not stable during March. On days 62 and 65, the cross-over appears to be weakening. The cold SSW moved along the northeast edge of the bank between the 100 and 200 m isobaths, with a small stream crossing the 100 m isobath and flowing to the NEP. On day 76, the cross-over appears to have intensified and can be clearly observed in SST data. Two days later, the cold-water patch covered almost half of the NEP area. This cold water patch

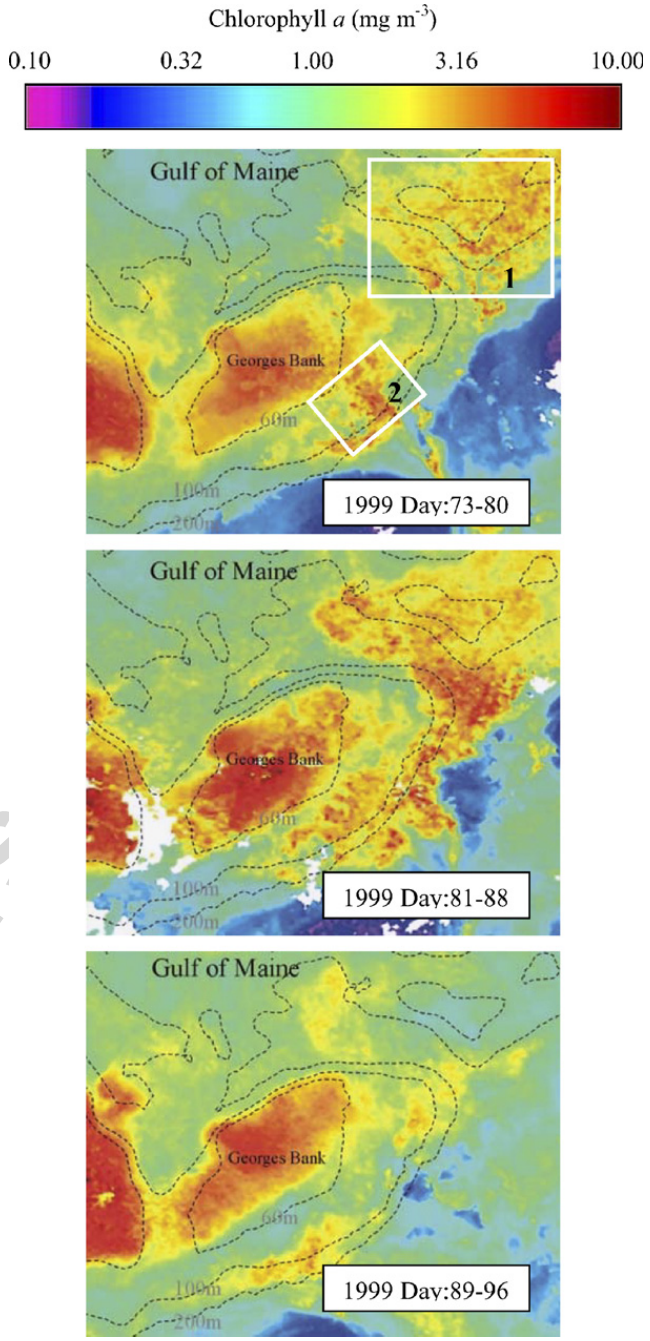

Fig. 1. Eight-day composite SeaWiFS image of GB and surrounding area during March 1999. Image is adapted from Dr. Andrew Thomas's website at the School of Marine Sciences, University of Maine.

disappeared by the end of March, as shown in the SST image of day 89.

2.2. CTD profiles

Unlike satellite images, which can only report the surface concentration of chlorophyll *a* and water temperature, CTD measurements are able to detect

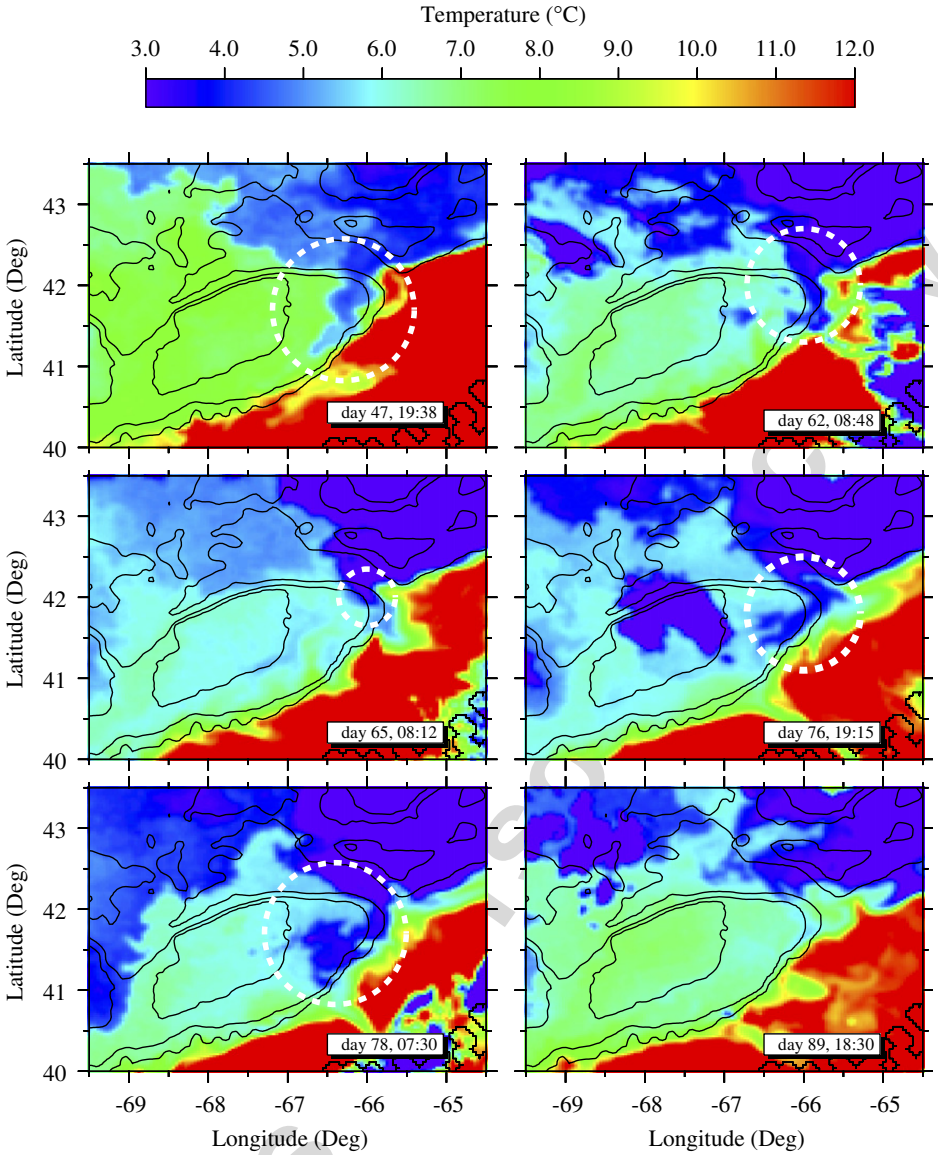

Fig. 2. Selected sea surface temperature (SST) images of GB and surrounding area during March 1999. Data are downloaded from the NOAA AVHRR (advanced very high resolution radiometer) website. White circles highlight SSW intrusion.

vertical profiles of physical and biological components in the water column. During the GLOBEC/GB broad-scale surveys, CTD measurements were conducted at stations covering the entire bank as shown in Fig. 3. Here we briefly present the temperature, salinity, and fluorescence profiles taken in March 1999 at the stations along a path from the NEC to the southern flank of the bank indicated by the connected arrows in Fig. 3.

Fig. 4 shows that the surface waters (<30 m depth) of the eastern-most station (25) had a temperature of about 3 °C and a salinity of about 31.7 PSU. This low salinity (<32 PSU) is a distinct signature of SSW, which confirms the feature

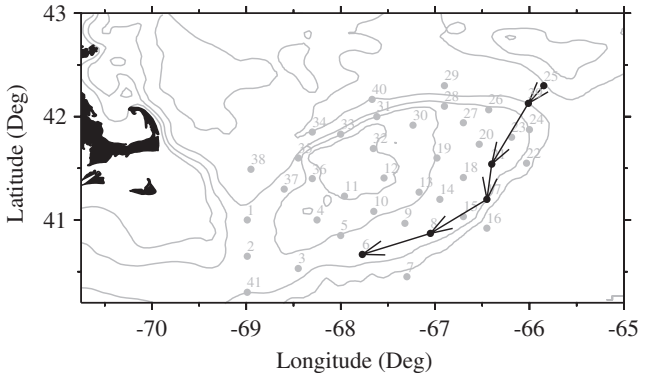

Fig. 3. The US GLOBEC/GB Program broad-scale sampling station plan for 1998 and 1999. CTD and water sample data at stations along the connected arrows are presented in Fig. 4 and 5.

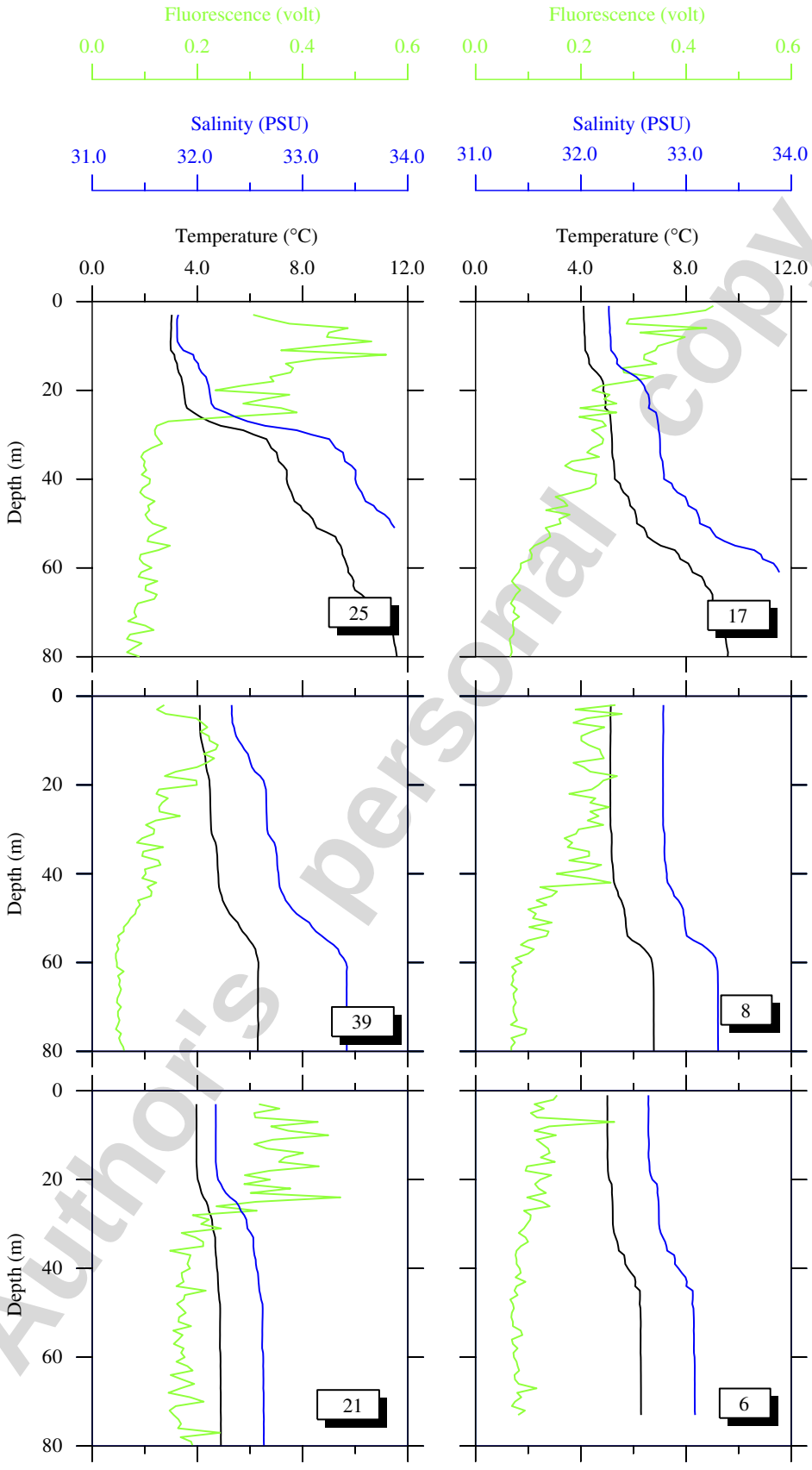

Fig. 4. Vertical profile of fluorescence (green lines), salinity (blue lines) and temperature (black lines) at the stations shown in Fig. 3 during March 1999.

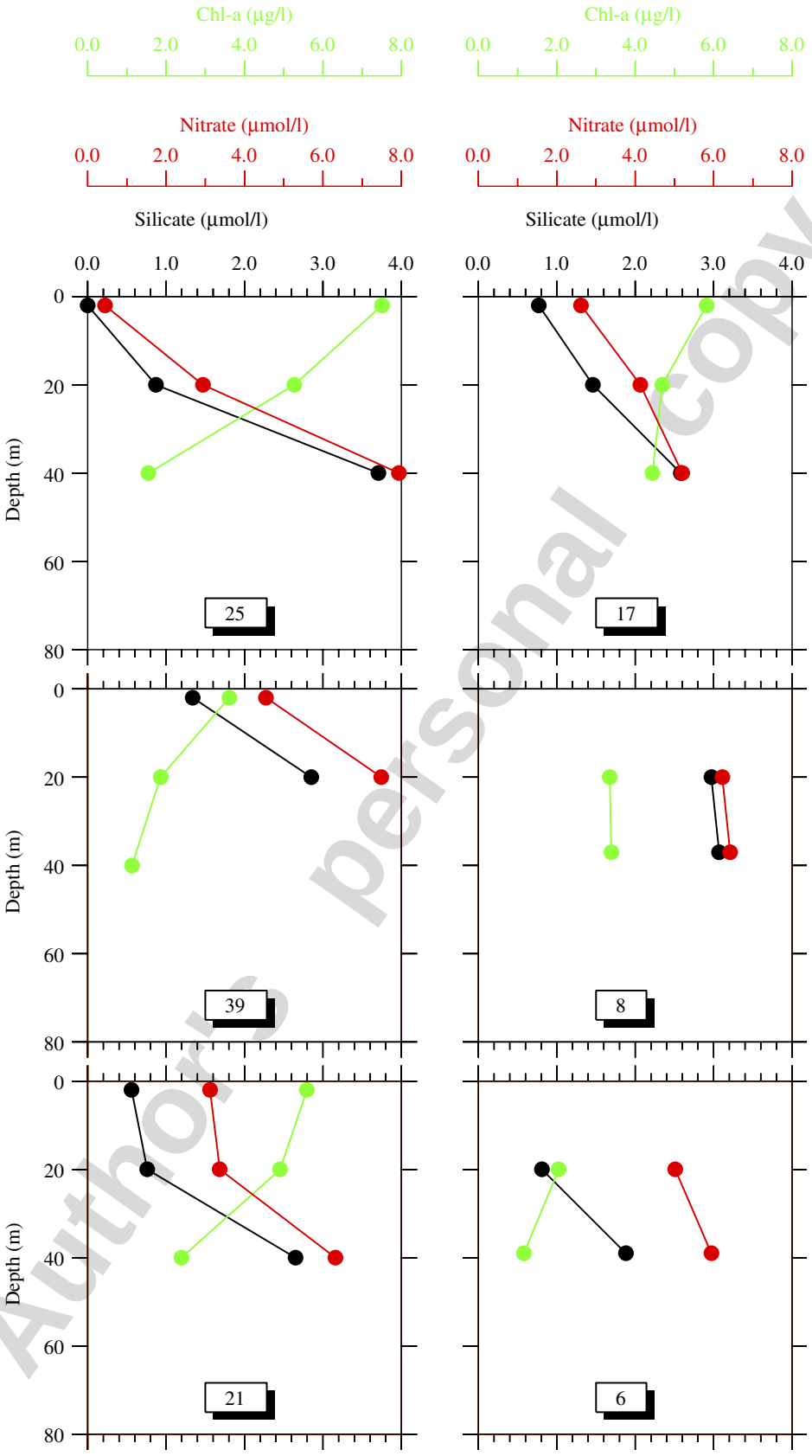

Fig. 5. Vertical profile of chlorophyll *a* (green dots), nitrate (blue dots) and silicate (black dots) at the stations shown in Fig. 3 during March 1999.

observed in the SST data. The temperature and salinity quickly increased at water depths >30 m. Waters >60 m at this location had a high temperature (>10 °C) and high salinity (>34 PSU), most likely of slope water origin. Accompaning this *T–S* structure, fluorescence data showed higher values at the surface (<30 m) and decreased sharply below.

Across the NEC, Station 39 showed that the surface salinity had increased to 32.4 PSU, and surface temperature was about 4 °C; the halocline has deepened from 30 m to about 50 m. Correspondingly, the fluorescence profile showed lower values in the surface water above 50 m, hence a less significant vertical gradient.

Further south of the bank, Station 21 showed a weaker temperature and salinity cline at ~30 m, although the fluorescence vertical gradient remained distinct. Station 17 is located on the outer edge of the bank. A weak halocline existed at a depth of 20 m, probably as a result of SSW intrusion. A much stronger halocline can be observed around 50 m. This halocline most likely reflects the boundary between the shelf water and slope water.

Continuing southward, the halocline and vertical gradient of fluorescence are still evident at 60 m at Station 8. However, at Station 6, the water column seems more vertically well mixed, and the vertical gradient of fluorescence had disappeared.

2.3. Water samples

Water samples were collected when the CTD measurements were taken for each station during the broad-scale survey. Here we present in Fig. 5 the observed vertical structure of chlorophyll *a*, nitrate and silicate concentration. The concentrations of chlorophyll *a* in the water samples are consistent with the CTD fluorescence data except that the vertical resolution is much coarser, with only three samples being collected in the entire water column.

In contrast to the high concentration of chlorophyll *a*, the concentrations of nitrate and silicate at the surface of Station 25 were nearly undetectable, and increased with depth. The concentrations of nitrate and silicate reached 8.0 and 3.7 μmol/l, respectively, at a depth of 40 m. This vertical distribution suggests that a significant phytoplankton bloom was taking place at the surface.

A trend of decreasing nutrient concentrations and increasing chlorophyll *a* in the surface layer was observed at Stations 39, 21 and 17 to some extent. Stations 8 and 6 have no data at the very surface, making it difficult to infer the vertical structures of the chlorophyll *a* and nutrients at those two stations.

3. Modeling approach

3.1. Physical model

The three-dimensional physical sub-model used in this study is the finite volume coastal ocean model (FVCOM), which was developed by Chen et al. (2003a) and applied to the GOM/GB region. The numerical domain of this model covers the entire GOM region and GB, enclosed by an open boundary running from the New Jersey shelf to the Nova Scotia shelf (Fig. 6). The horizontal resolution of the model grid is about 3–4 km around the coast and edge of GB, and about 5–8 km in the interior of the GOM and near the open boundary. In the vertical, a uniform σ coordinate grid is used, with vertical resolution $\Delta\sigma = 0.0323$ (31 points in the vertical). This resolution corresponds to 1.3–4 m vertical resolution over the depth range of 40–120 m on GB and a 10 m spacing over the off-bank depths of 300 m. Mellor and Yamada's (1982) 2.5 turbulence closure scheme is used for the turbulent mixing of momentum and tracers. This is the same scheme used in the ECOM-si model (Blumberg, 1994).

The model was forced along the open boundary by the surface semidiurnal (M_2, S_2, N_2) and diurnal (O_1 and K_1) tidal elevations and phases. The sea-level data used for tidal forcing were interpolated from the results of the Egbert et al. (1994, 2002) 1/6° inverse tidal model. A gravity–wave radiation condition on currents was applied at the open boundary to minimize energy reflection into the computational domain. The surface and bottom boundary conditions for both momentum and biology are the same as in ECOM-si and described in Ji et al. (2006). Surface heat and wind data were obtained from the GOM/GB regional mesoscale meteorological model MM5 (Chen et al., 2005).

3.2. Numerical experiments

In order to obtain a preliminary assessment of paths and time scales of water parcel movement, a Lagrangian particle trajectory program was incorporated into FVCOM. The technique, originally developed by Chen and Beardsley (1998) for use with ECOM-si, was subsequently modified for FVCOM. In this program, particle trajectories are

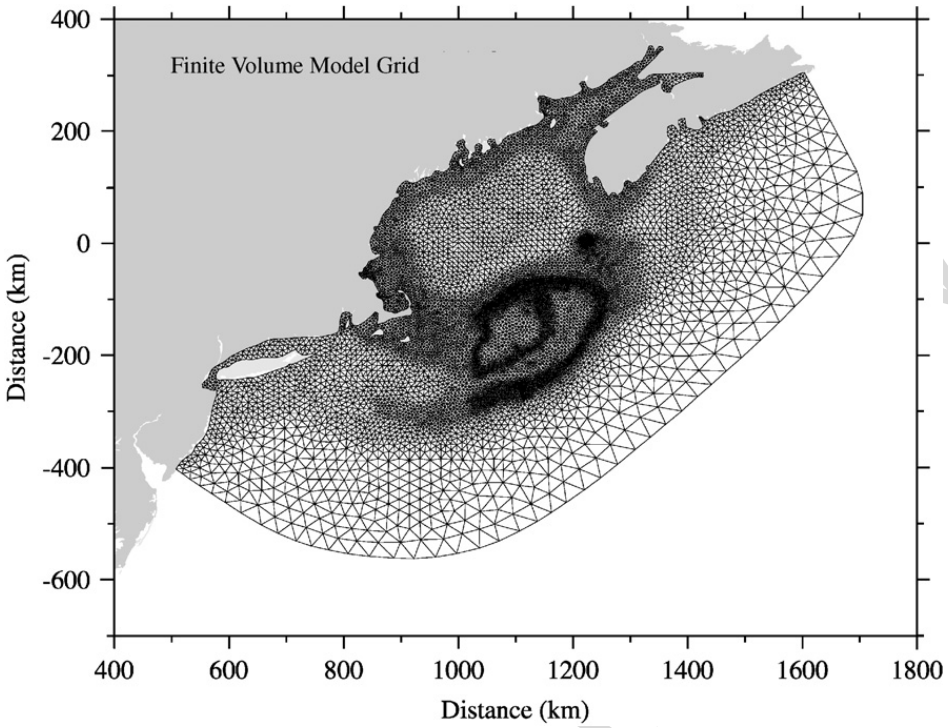

Fig. 6. FVCOM unstructured numerical model grid for GOM/GB region.

traced by solving the equation

$$\frac{d\vec{x}}{dt} = \vec{v}(\vec{x}(t), t),$$

where $\vec{x}(t)$ is the particle position at a time t and $\vec{v}$ is the velocity interpolated from the surrounding model grid points. Horizontally the velocity is interpolated using a least squares method based on velocities at four adjacent cell points, while a linear interpolation is used in vertical. The equation is solved by a classical 4th order 4-stage explicit Runge–Kutta method with a time step of two minutes and a truncation error of the order $(\Delta t)^5$.

The particle trajectory experiments can provide insights into the basic Lagrangian kinematics but do not include the effect of diffusion. To examine the influences of both advection and diffusion on the transport of phytoplankton, passive tracer experiments were conducted, with tracer injected into two regions. One was in the central portion of the bank inside the 60 m isobath, with a tracer concentration of 1 (relative concentration, dimensionless) over the entire water column. The other is near the Browns Bank area with a tracer concentration of 1 (relative concentration, dimensionless) in the surface waters from 0 to 30 m.

The biological model was that used in the 1-D and 2-D models (Ji et al., 2006). The coupled biological and physical model was started at the beginning of January 1999 and run until February 28, with a horizontally and vertically homogenous distribution of biological variables as follows: nitrate: 5.0 μmol N/l; ammonium: 0.1 μmol N/l; silicate: 5.0 μmol Si/l; small phytoplankton: 0.1 μmol N/l; large phytoplankton: 1.0 μmol N/l; small zooplankton: 0.1 μmol N/l, large zooplankton: 0.2 μmol N/l; detrital nitrogen 5.0 μmol N/l; detrital silicon: and 2.0 μmol Si/l. The model results for February 28 served as the initial condition for the model run of March 1999.

4. Model results and discussions

4.1. Physical fields

The modeled subtidal currents on GB are the result of the combined effects of several processes, including tidal rectification, wind- and baroclinic forcing. To remove the basic tidal constituents, a 40-h low-pass filter is applied to obtain the subtidal currents. The GOM/GB MM5 model surface wind fields show mesoscale spatial structure and 5–7 D temporal variations (Fig. 7). As shown in the following section, the wind fields appear to be closely related to the surface circulation pattern on

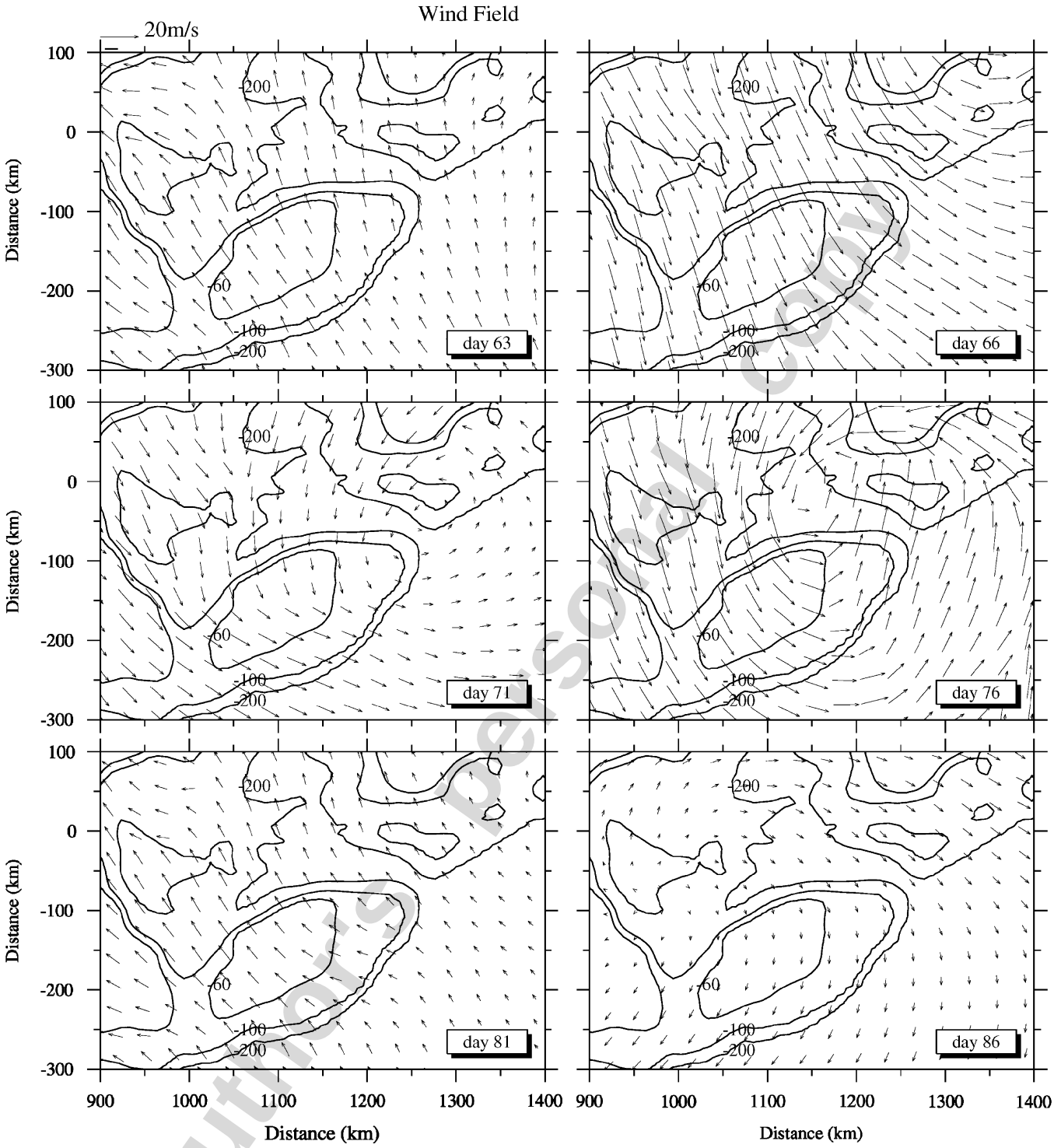

Fig. 7. Surface wind fields on selected days in March 1999 from the GOM/GB MM5 model output.

GB and the occurrence of SSW "cross-over" events during this time of the year.

The surface subtidal currents showed a strong relationship with wind forcing. For example, on day 66 (Fig. 8, upper panel), the surface waters over most of GOM and GB were dominated by southward subtidal currents, corresponding well with the prevailing southeastward wind field during that time. The velocity of these subtidal currents reached 30 cm/s. This surface flow structure persisted until day 76 (Fig. 9, upper panel) when a meso-scale low (cyclonic eddy) developed north of

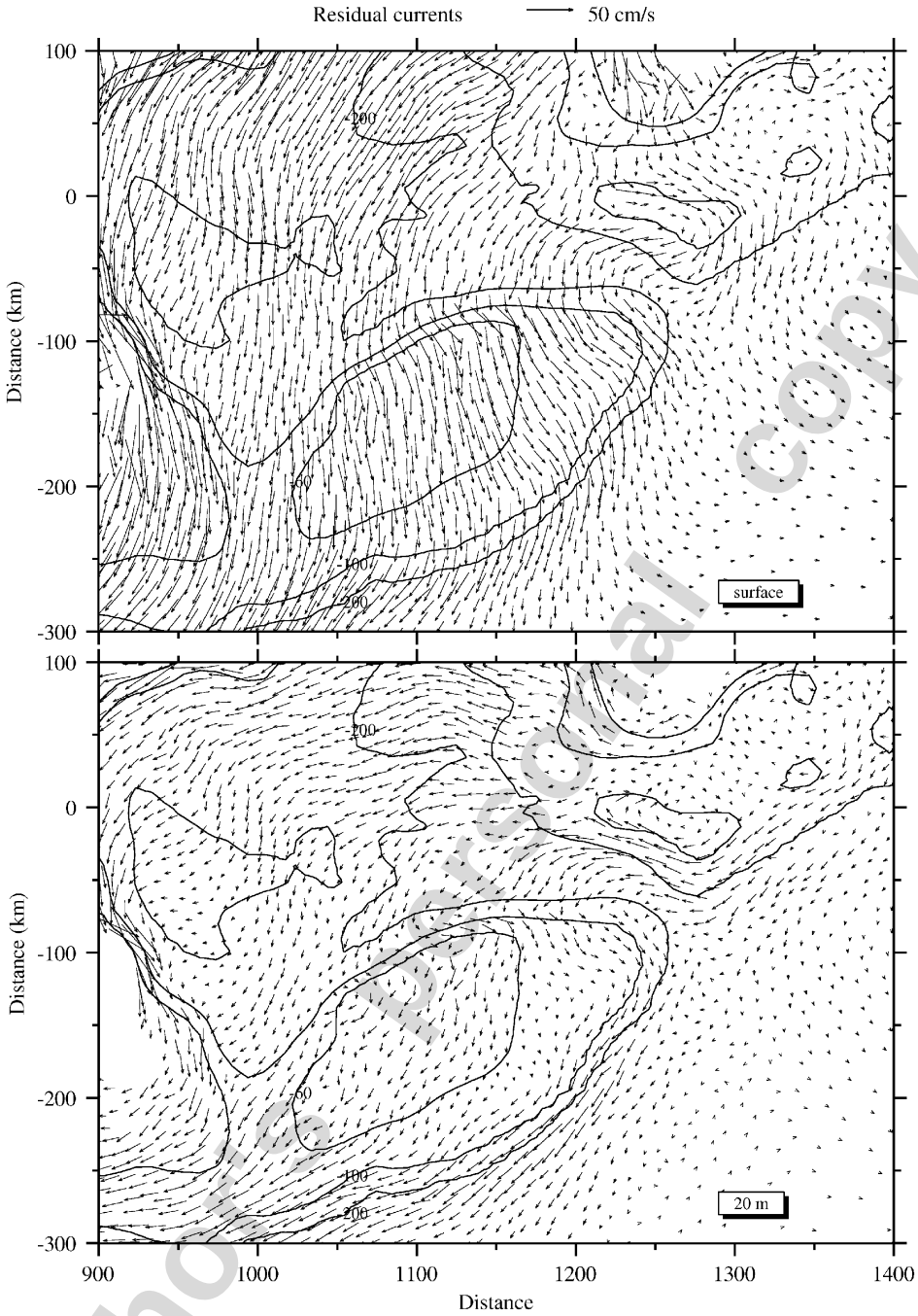

Fig. 8. Model-computed subtidal currents on GB and surrounding region on day 66. upper: surface subtidal currents; bottom: subtidal currents at 20 m water depth.

GB (Fig. 7). The surface subtidal currents at that time were relatively weak in the GOM region and the central portion of the bank, except for the northern and the southern flanks of the bank. On day 81 (Fig. 10), the surface subtidal currents shifted northeastward, and the jet current along the northern flank was intensified, while the jet current on the southern flank was significantly weakened.

The subtidal currents at 20 m were less affected by wind forcing. The most significant feature of the circulation is the clockwise flow around the bank (Figs. 8, 9 and 10, bottom panels). For example, on day 76, the jet current reached 20–30 cm/s along the edge of the northern flank. The flow then turned southward at the edge of the NEP and then turned more southwestward and widened. The velocity was 20–30 cm/s near the 200 m isobath and decreased to

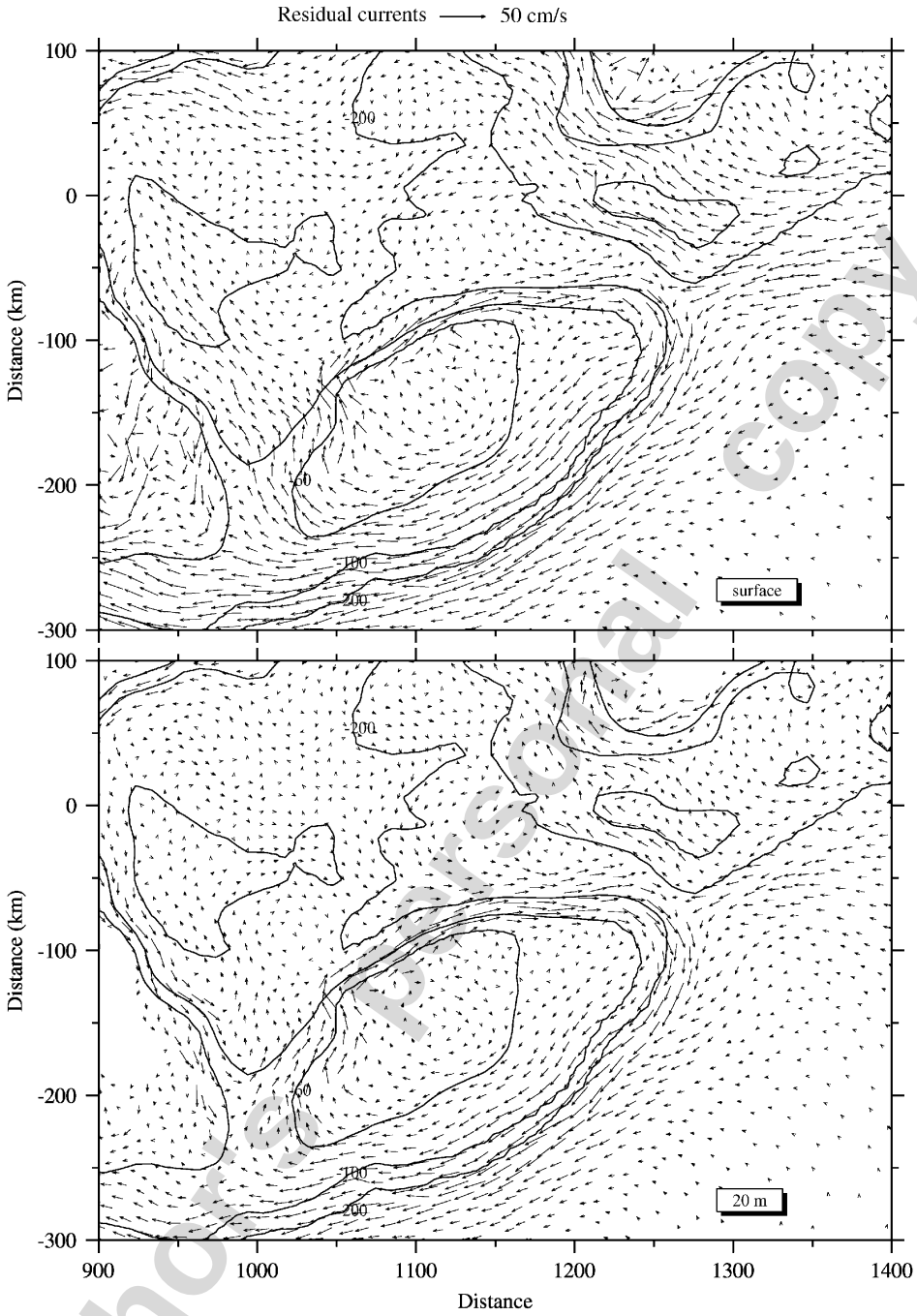

Fig. 9. Model-computed subtidal currents on GB and surrounding region on day 76. upper: surface subtidal currents; bottom: subtidal currents at 20 m water depth.

5–10 cm/s both onbankward and slopeward. This result is slightly different from that of (Chen et al., 2003b) using ECOM-si (which was initiated with climatological temperature and salinity fields and driven by the M_2 tidal components only), where two major flows circulated around the bank. The first flow was the tidally-induced, topographically-controlled clockwise subtidal circulation found around the crest of the bank, where a strong eastward/southeastward current jet of 15–18 cm/s formed along the edge of the northern flank and a relatively weaker and wider westward flow of 5–8 cm/s in the region deeper than 60 m on the southern flank. The second flow was a buoyancy-induced, westward mean current located near the 100 m isobath at the shelf break of the southern flank. In the results of the present FVCOM model, the two flows on the southern flank are hard to

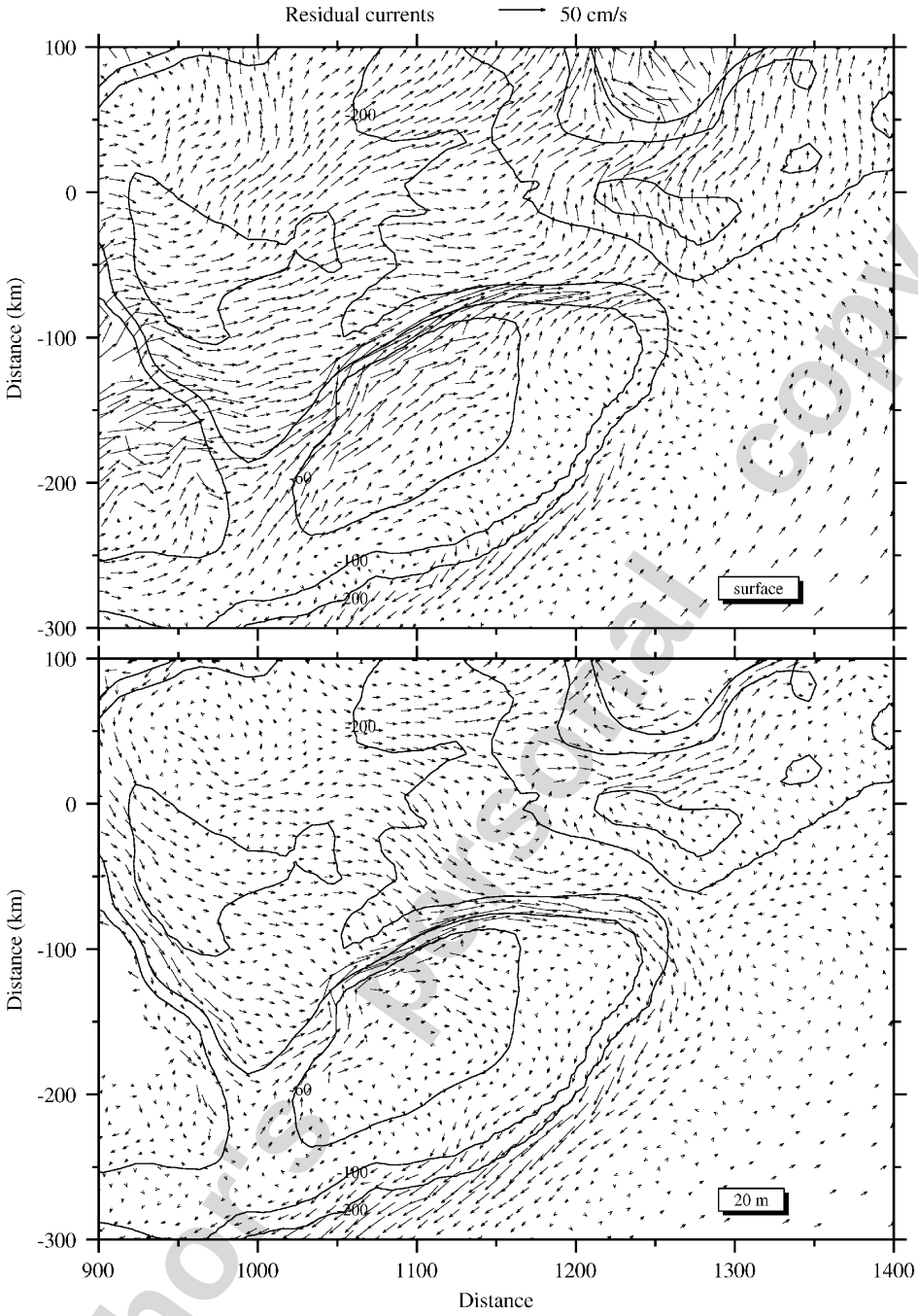

Fig. 10. Model-computed subtidal currents on GB and surrounding region on day 81. upper: surface subtidal currents; bottom: subtidal currents at 20 m water depth.

separate, which could be caused by the different wind forcing and initial conditions of both temperature and salinity used in these two different hydrodynamic models.

4.2. Lagrangian particle trajectory

Particles were released from two different locations, one in a square area including Browns Bank and surroundings (Fig. 11, day 63, referred as Area A hereafter), and the other in the central portion of the bank inside the 60 m isobath (Fig. 13, day 63, referred as Area B hereafter). Trajectories were traced from day 63 to day 86. For particles released from Area A (Fig. 11), only a few particles flowed onto the bank by day 66. By day 71, 25% of particles were inside the 200 m isobath of the bank. After the particles flowed onto the bank, they

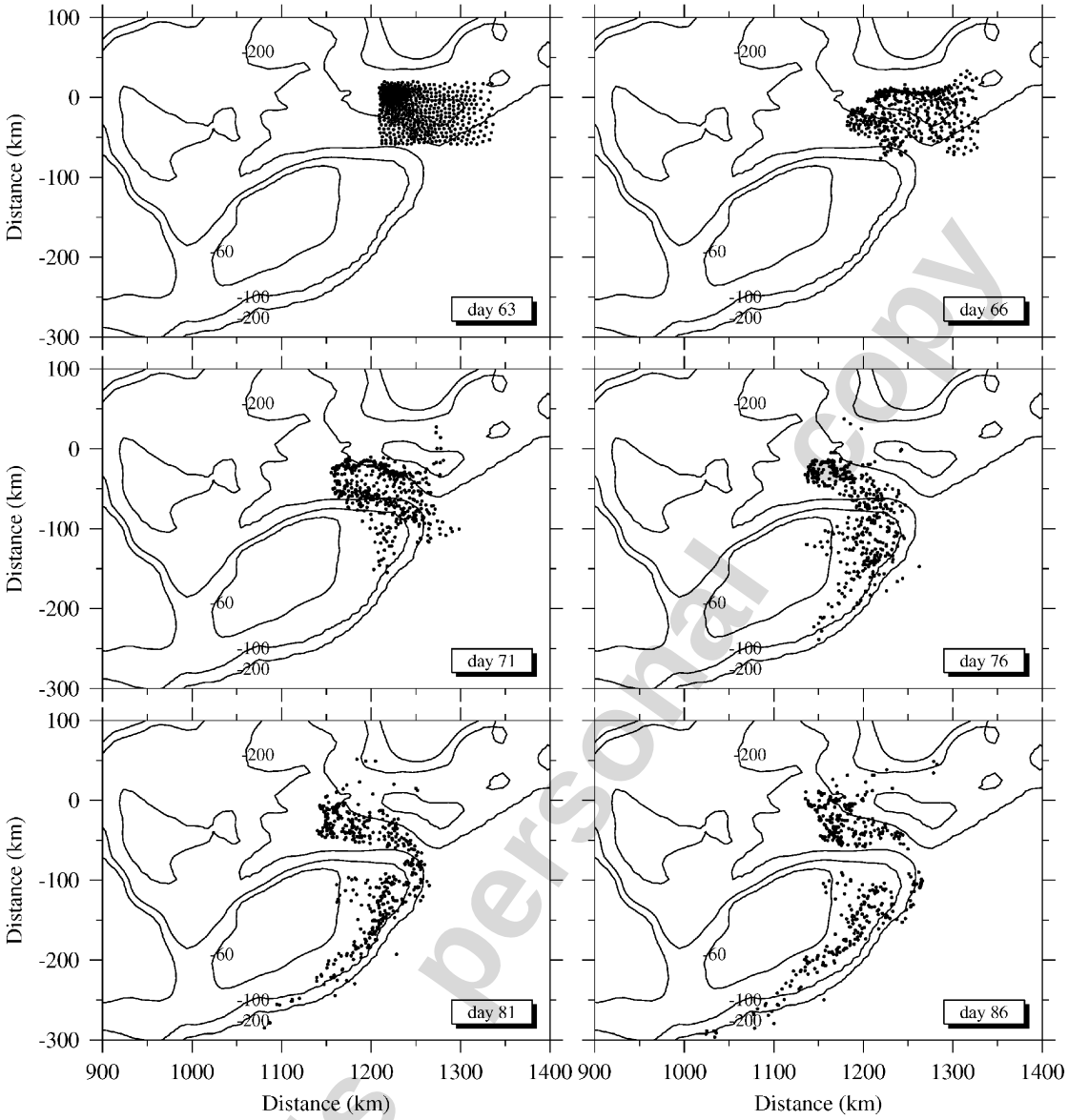

Fig. 11. Selected snapshots of Lagrangian particle trajectories. Particles were released at the surface near Browns Bank on day 63.

moved southwestward following the clockwise circulation. More particles arrived on the bank on day 76, accounting for ~45% of the total particles. After that, the particles seemed to separate into two groups as shown on days 81 and 86, with one group remaining in the NEC and the other moving around the southern flank. The velocity of this movement decreased after day 76. Overall, ~48% of the total particles arrived inside the 200 m isobath of the bank in 23 days. The movement of particles at the surface was strongly related to the surface subtidal current, which in turn was related to the surface wind stress. The particles released at subsurface (30–40 m below the surface) of Area A were less likely to be transported to the bank (Fig. 12). Most of them moved northwestward, with only a few flowing onto the bank, suggesting that a strong velocity shear existed between surface and subsurface. This velocity shear caused the particles at different depths to follow difference paths.

The particles released at the surface of Area B were quickly "washed out" (Fig. 13), with only 11% of particles remaining inside the 60 m isobath on day 71, and none on day 81. The particle trajectories corresponded well with the wind stress. Most of the particles moved southward (Fig. 13, day 66, 71), converged on the southern flank, and then moved southwestward and out of the model domain (Fig. 13, days 76, 81 and 86). The particles released subsurface (20–30 m below the surface) of

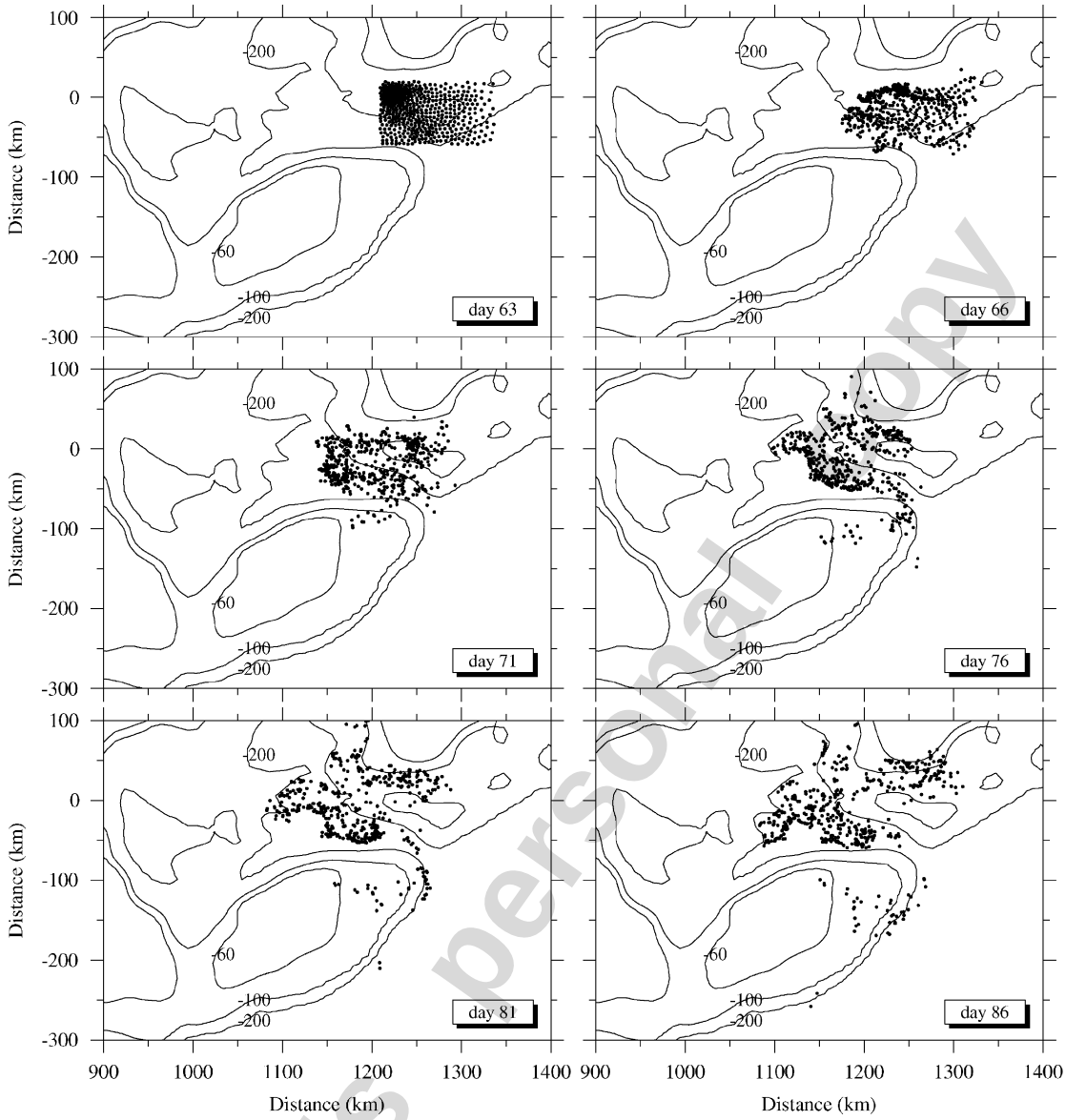

Fig. 12. Selected snapshots of Lagrangian particle trajectories. Particles were released sub-surface (30–40 m below the surface) near Browns Bank on day 63.

Area B were less likely to leave the central portion of the bank in comparison with the surface ones. As shown in Fig. 14, after 23 model days, only 21% of the total particles had moved outside the 60-m isobath, flowing either northward to the northern flank of the bank or southwestward to the Great South Channel. None of the particles arrived on the southeastern or southern flank of the bank during the model time period (Fig. 14, bottom right panel).

The particle trajectory experiments indicate that particles at the surface of both Areas A and B can move to the southern flank, but subsurface particles generally do not. To further quantify the water parcel movements, including diffusion processes, the results of tracer experiments are presented next.

4.3. Tracer movement

Tracer was "injected" homogeneously into the surface layer (<30 m) of Area A and the whole water column in Area B. For Area A, two different vertical mixing coefficients were applied to test their effects on the cross-over events: Case 1 represented the baseline model run without changing the vertical mixing coefficient, while Case 2 had a smaller vertical mixing coefficient in the water column below 30 m depth.

Case 1: The surface tracer initialized in Area A decayed very quickly (Fig. 15). The initial concentration on day 63 was 1.0 unit/l. On day 76, some tracer cross-over towards the NEP

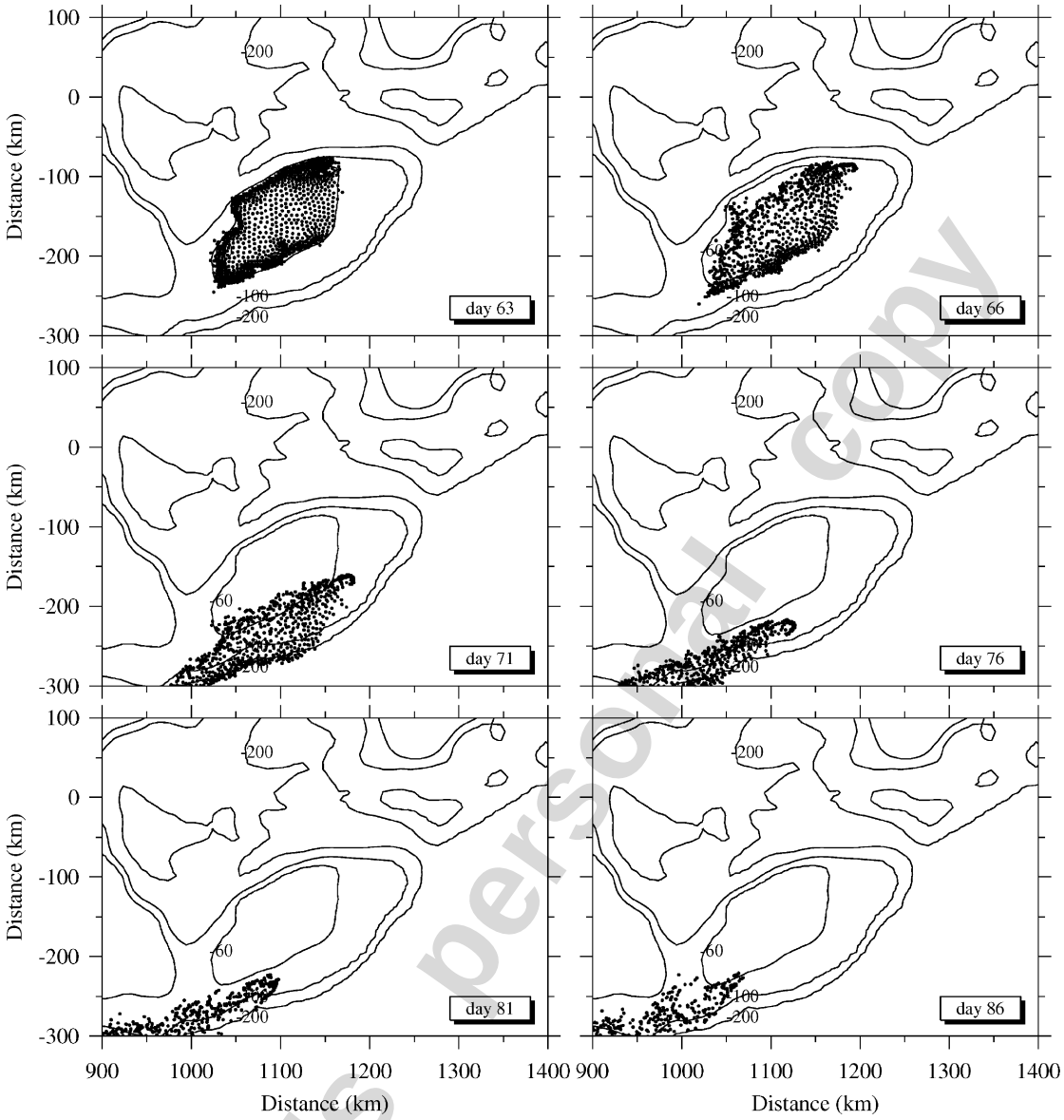

Fig. 13. Selected snapshots of Lagrangian particle trajectories. Particles were released at the surface on the central portion of GB on day 63.

can be seen, although the concentration had already declined to <0.3 unit/l. On day 86, the tracer concentration on GB diminished to near zero.

Case 2: If the tracer initialized in Area A was subjected to less vertical mixing between surface (above 30 m) and deep waters (below 30 m), much more tracer crossed-over to the bank (Fig. 16). In this case, the pattern of the tracer movement was much more similar to the particle trajectories, which showed a significant number of particles crossing-over and flowing to the southeastern and southern flanks of the bank.

Fig. 17 shows that the model conserves tracer, i.e., the integral of tracer concentration over the entire model domain is constant except for small perturbations caused by numerical error (as shown in the bold solid line). The integration of tracer below 30 m water depth kept increasing with time, reaching over half the total concentration in Case 1 and much less in Case 2. This supports the suggestion that the vertical mixing loss of the tracer from the surface layers caused the differences in horizontal distributions shown in Figs. 15–16.

The tracer initialized in Area B (Fig. 18) showed a relatively slower decay compared to Case 1. The maximum concentration on the top of the bank remained >0.8 unit/l after 20 model days. This is not a surprise result since the tracer was initiated

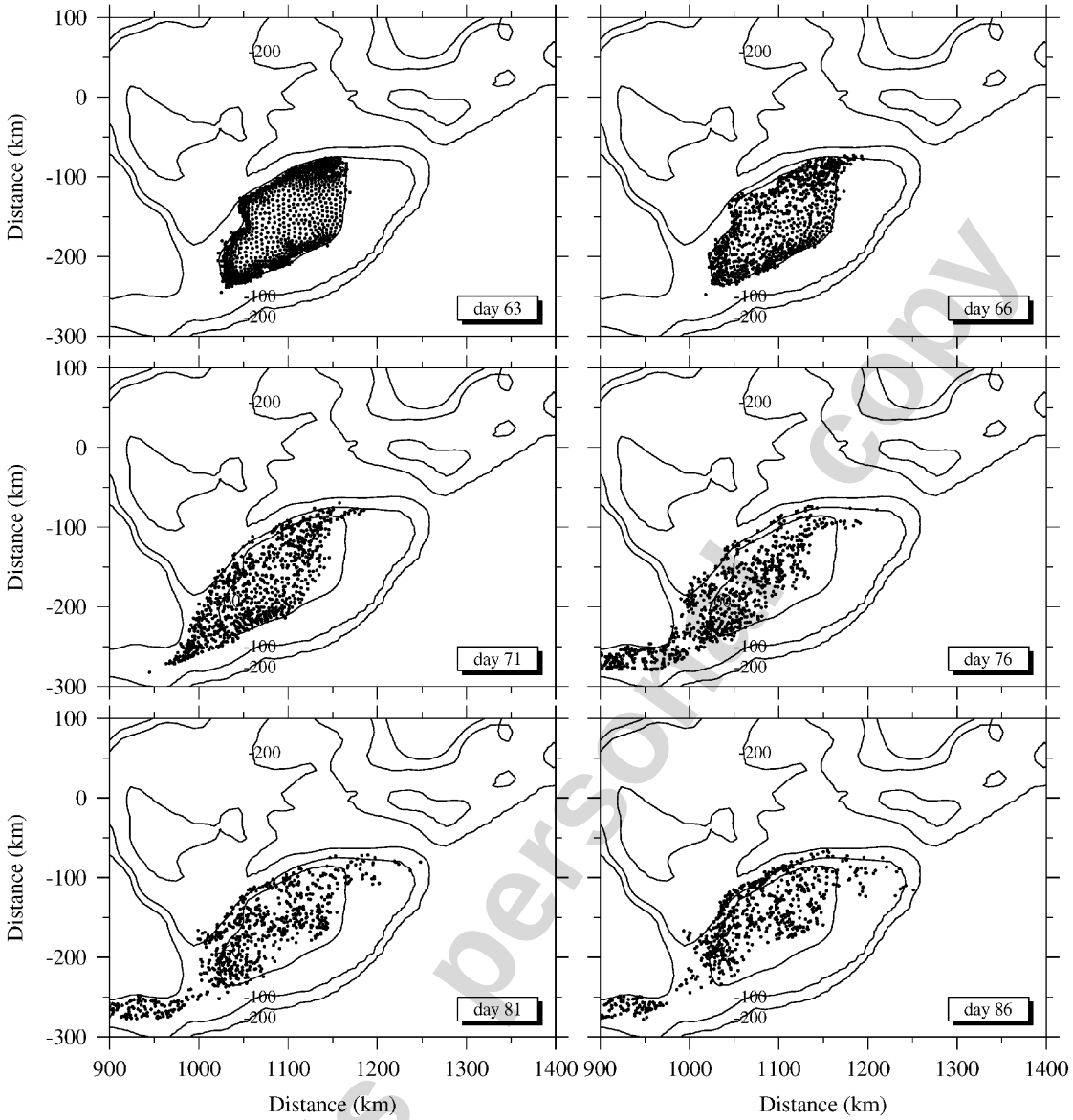

Fig. 14. Selected snapshots of Lagrangian particle trajectories. Particles were released subsurface (20–30 m below the surface) on the central portion of GB on day 63.

uniformly from bottom to surface, so there was no dilution caused by vertical mixing. As shown in the progressive movement of tracer (Fig. 18, day 63–86), most of the tracer drifted southwestward and left the model domain, without a detectable movement towards the southeastern and southern flanks during the model time period.

4.4. Coupled biological modeling results

Unlike the passive tracer, the coupled biological–physical model included biological source and sink terms. This model experiment was intended to examine whether a phytoplankton bloom could extend from Area A to the southeastern and southern flanks of GB under the standard model configuration. In order to focus on bloom dynamics, only the results for large phytoplankton are presented here. The model was initialized with the biological field in the whole model domain as specified in Section 3.2. Such an initial condition provides a basic background field, with stabilized horizontal and vertical distributions of biological variables. It was also assumed that there was an ongoing phytoplankton (diatom) bloom in the Area A, with the concentration of large phytoplankton specified as 3 μmol N/l (equivalent to 6 μg Chl-*a*/l with N:Chl-*a* = 2.0).

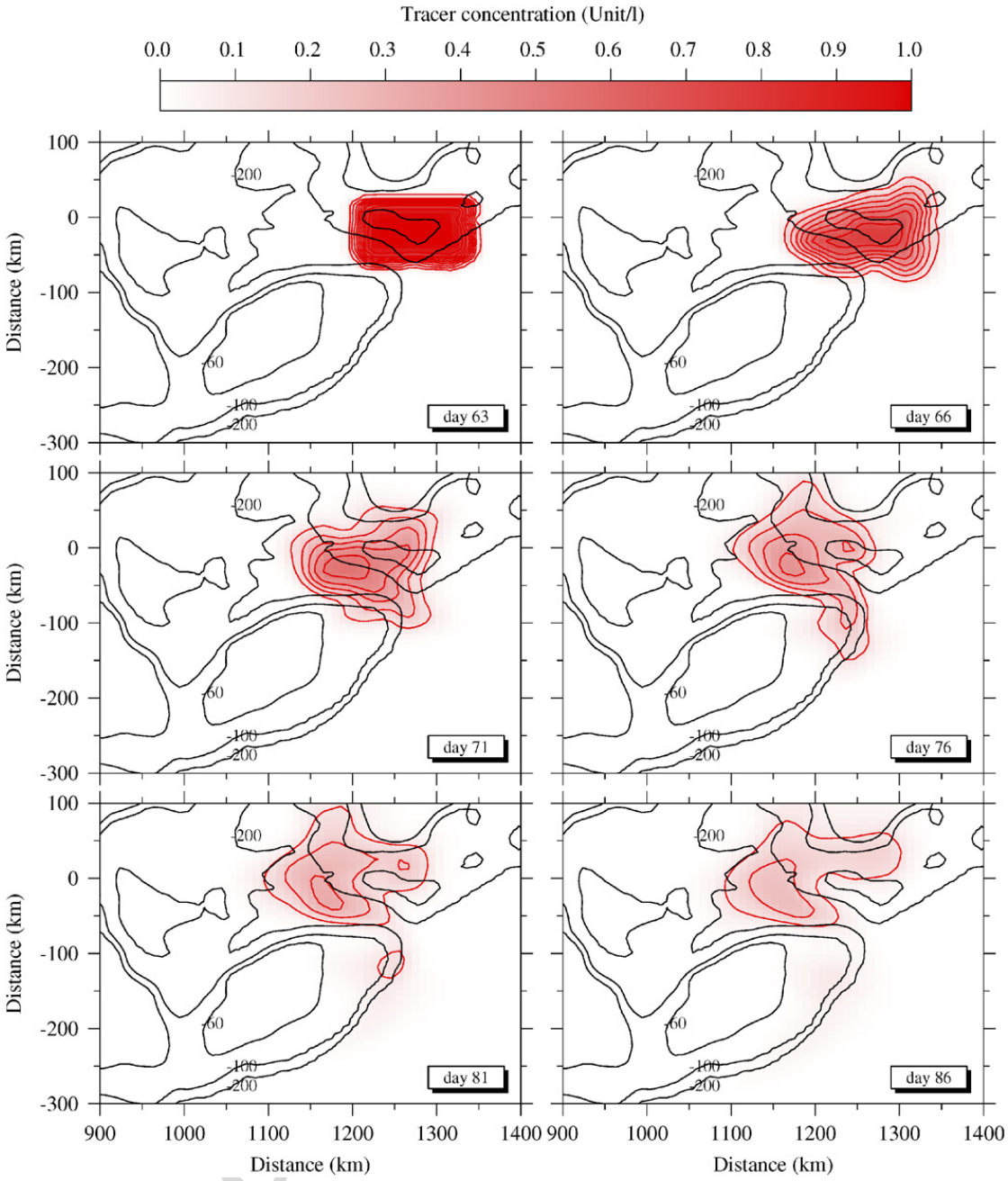

Fig. 15. Selected snapshots of tracer experiment results. Tracer were released in the surface layer (<30 m) near the Browns Bank region at day 63.

Fig. 19 shows that the movement of the bloom patch was similar to that of the tracer experiments during days 66–76. An increase of large phytoplankton at the surface occurred outside the 100 m isobath on the southeastern flank from day 81 to 86. This result explains the appearance of the phytoplankton bloom along the southern edge of the bank near the shelf-break front. From the flow field of the hydrodynamic model, it is clear that the clockwise jet along the shelf break extended outside of the 200 m isobath, indicating that the shelf-break front was probably related to the distribution of water containing the phytoplankton bloom. The use of climatological data to initialize temperature and salinity in this model may cause a shift (outward) of the shelf-break front and therefore a mismatch of the location of the phytoplankton bloom between the model and observations. That's probably the reason why the model did not reproduce the phytoplankton patches observed on the southeastern and southern flanks between the 60 and 100 m isobaths.

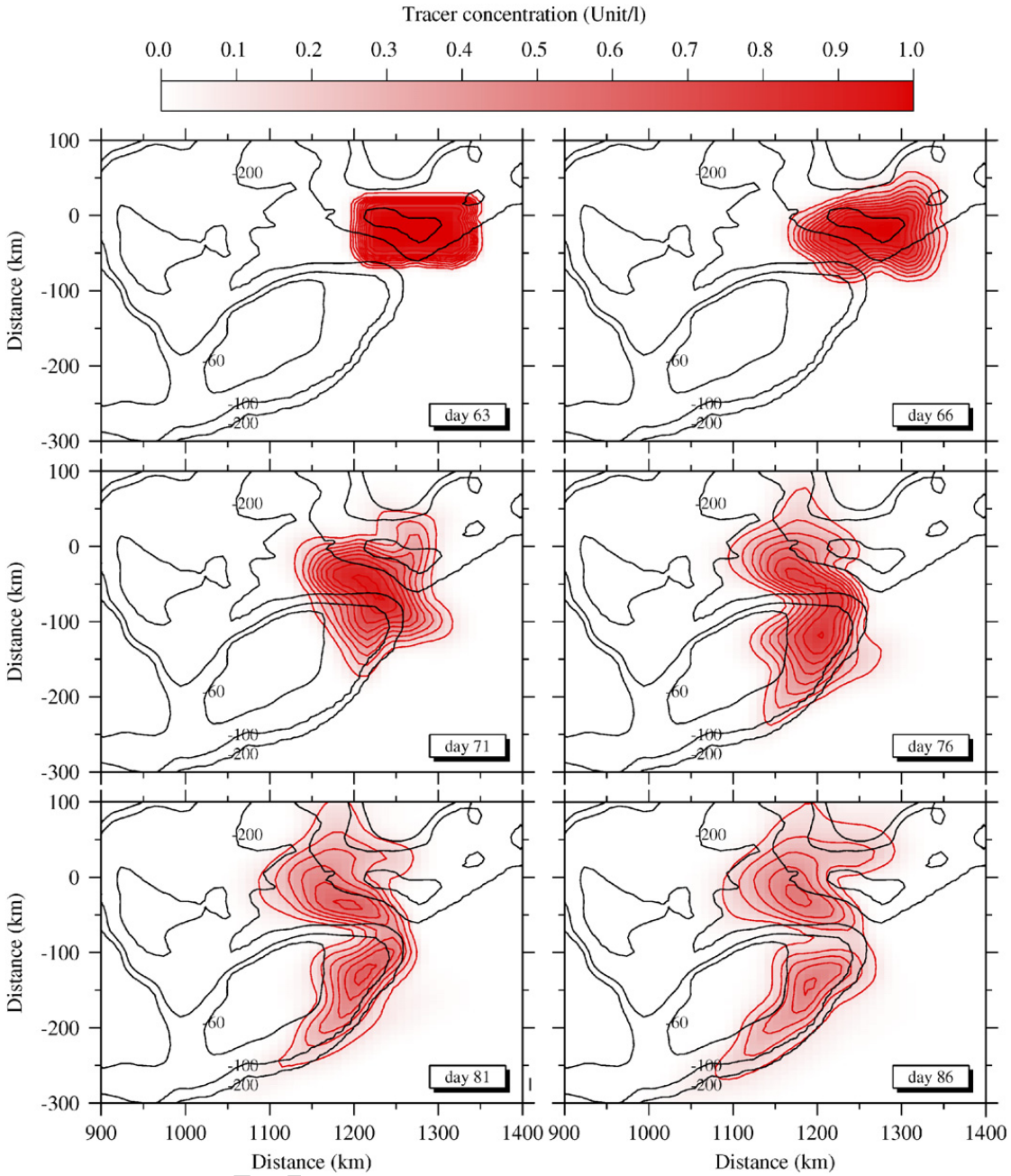

Fig. 16. Selected snapshots of tracer experiment results. Tracer was released in the surface layer (<30 m) near the Browns Bank region at day 63. The vertical mixing coefficient in the water column below 30 m is one order smaller than the standard model run shown in Fig. 15.

The results of the 3-D coupled biological–physical model were affected by many factors, including the initial and boundary conditions of the biological variables. In this model, a high concentration of large phytoplankton in SSW patch was specified to represent an on-going phytoplankton bloom. The initial concentrations of other biological variables were not available; therefore the results of this numerical experiment need to be interpreted carefully with regard to its sensitivity to any perturbation in the initial conditions. Nevertheless, the model results suggest that it is possible for the water containing a bloom to maintain its high concentration of phytoplankton while it is subjected to both horizontal and vertical advection and diffusion. Future modeling exercises with better initial and boundary conditions are necessary to obtain more realistic simulations of spring bloom and associated lower trophic food-web dynamics in the fully 3-D model domain. It requires a more realistic initial condition for all the biological compartments described in this model. Some

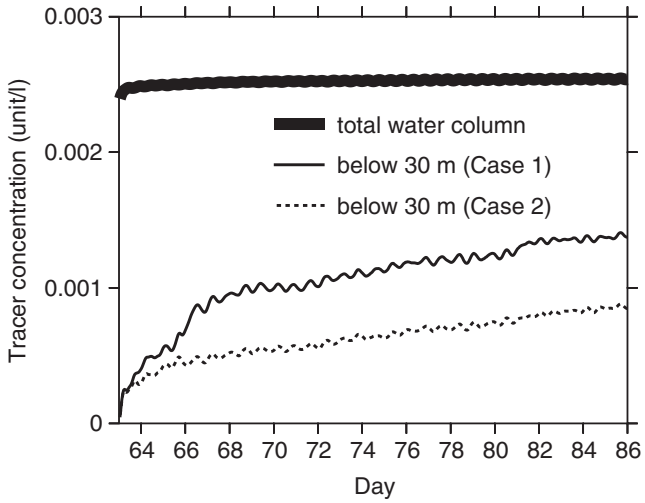

Fig. 17. Time series of vertically-integrated tracer concentration in the entire model domain.

of them might be obtained in a format of a climatological mean by a compilation of historical data (e.g., Petrie and Yeats, 2000) through out the GOM/GB region. Moreover, a better understanding of the boundary conditions in the upstream of the model domain near the Scotian Shelf will help to better define the incoming flux of biological compartments (e.g., nutrients and plankton).

4.5. *Sources of the phytoplankton bloom on the southern flank*

The blooms that occurred on the southern flank of the bank in March 1999, as shown in satellite images, were not likely a result of direct washout from the central area of the bank or from the SSW. Although the particle trajectory results show that transport from both areas is possible, vertical mixing prevents a substantial replacement of water on the southern flank with surrounding water. Tracer experiments exclude the possibility of direct washout from the central portion of the bank to the southern flank. For the SSW, the tracer can reach the southern flank and maintain $>80\%$ of its initial concentration only if the vertical mixing between the surface and deep waters is weak.

The separation of bloom patches shown in the satellite images between the southern flank and the NEC between days 73 and 80 suggests that the bloom on the southern flank is not likely an extension of the upstream bloom. Instead, the bloom may be triggered by in situ growth of phytoplankton, with the help of stratification induced by SSW cross-overs. Fig. 2 (upper left panel) shows that the cross-over can occur in February. This suggests that there was a time window for SSW to arrive on the southern flank and set up stratified conditions that were favorable for phytoplankton blooms. Such a widespread SSW influence over the southern flank between the 60 m isobath and the shelf break front was also observed in 1997 (Ryan et al., 2001). This SSW cross-over event might significantly change the location of the salinity front and hence the spring-bloom dynamics.

In contrast to the 1999 case, no detectable bloom occurred on the southern flank in March 1998. Patches with high phytoplankton concentrations appear on the top of the bank and in the slope water outside of the 200 m isobath. One possible explanation is that SSW cross-over was relatively weak that year. Therefore, there was no advectively forced setup of stratification to allow an early spring bloom on the southern flank. The CTD data (not shown here) indicates that the water was well mixed along the selected section, especially at Stations 21, 8 and 6, where water temperatures and salinities were vertically homogeneous. The fluorescence data at Station 8 also indicate that the phytoplankton did not show a higher concentration in the surface layer. The difference between 1998 and 1999 provides additional evidence showing the importance of SSW cross-overs on the spring phytoplankton dynamics on GB.

The influence on the spring bloom of slope water from the southern edge of the bank remains unclear. Previous studies have shown that the phytoplankton bloom could occur early at the shelf break front where shoaling of the mixed layer by the front locally increases light exposure (Marra et al., 1982; Malone et al., 1983). The interaction of warm-core rings of Gulf Stream origin with shelf water masses is one of the factors that influence water column stability and vertical flow in the shelf break front area (Smith and Baker, 1985; Yentsch and Phinney, 1985; Nelson et al., 1989; Ryan et al., 1999, 2001). However, this process is difficult to quantify, since it is intermittent in time and space. A 3-D model with a better open-boundary condition on the slope side would be necessary to study such influences.

4.6. *Biological importance of the spring bloom on the southern flank*

Many of the previous GB studies focused on the productivity of the central bank, stimulated by the dilemma of high primary productivity and low new

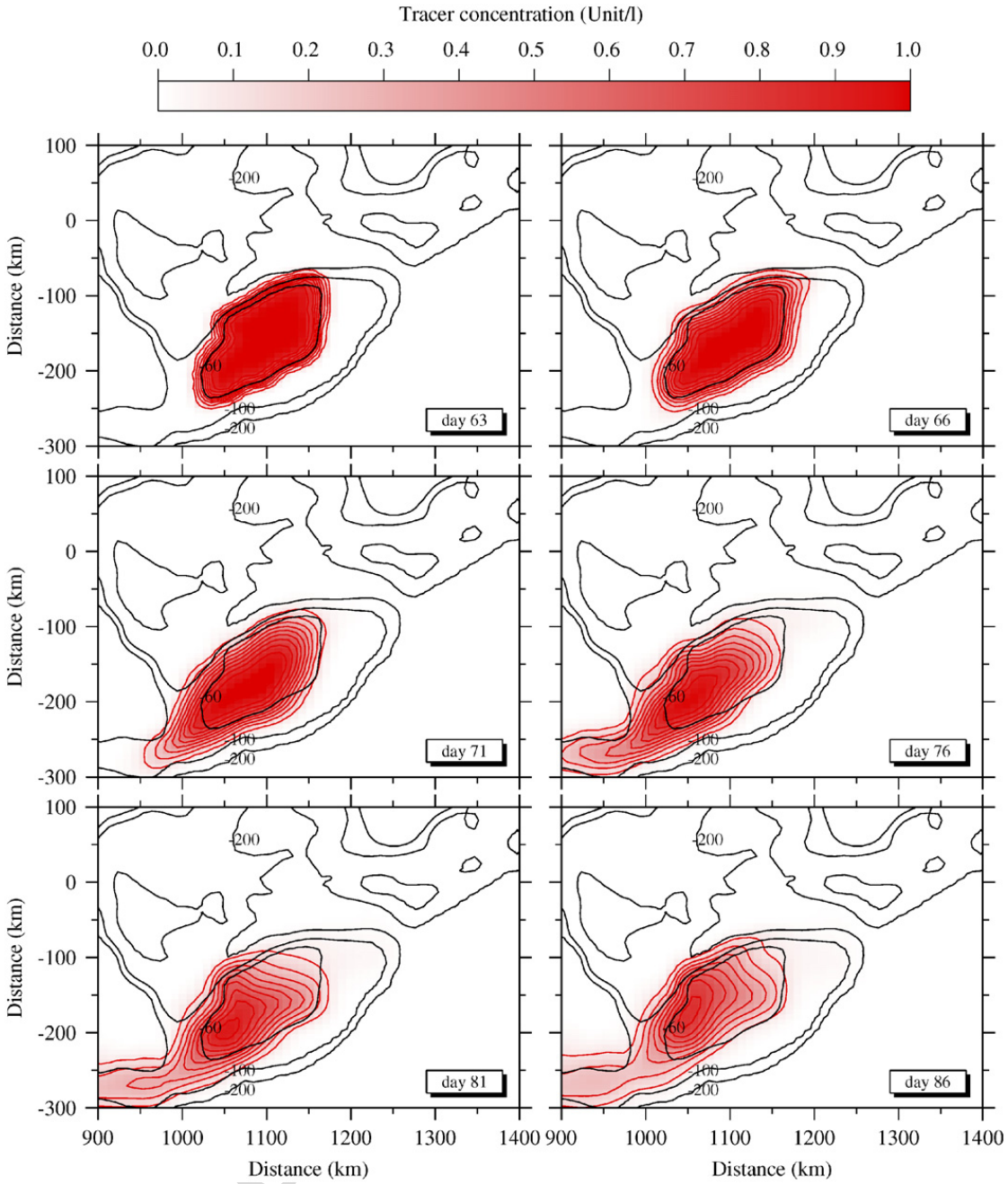

Fig. 18. Selected snapshots of tracer experiment results. Tracer was released uniformly in the entire water column of the central portion of GB at day 63.

nutrient supply in that region. These studies addressed the cross-frontal exchange of nutrients and the associated phytoplankton production (Franks and Chen, 1996, 2001; Chen and Beardsley, 1998, 2002; Houghton and Ho, 2001; Houghton, 2002; Chen et al., 2003b). Less attention has been paid to the dynamics of phytoplankton production on the southern flank, although this area is fundamentally important to the dominant zooplankton species, such as *C. finmarchicus*, during the spring and early summer. Both observational data (Meise and O'Reilly, 1996; Durbin et al., 2000) and modeling studies (Miller et al., 1998; Lynch et al., 1998) suggest that the southern flank is a major pathway and growth/reproduction area of *C. finmarchicus* when the population is advected from its GOM upstream home and moved around GB by the clockwise circulation.

Food limitation of *C. finmarchicus* is most likely to occur on the southern flank of the bank (Campbell et al., 2001). The timing of the spring bloom is influenced by advection from the GOM and Scotian

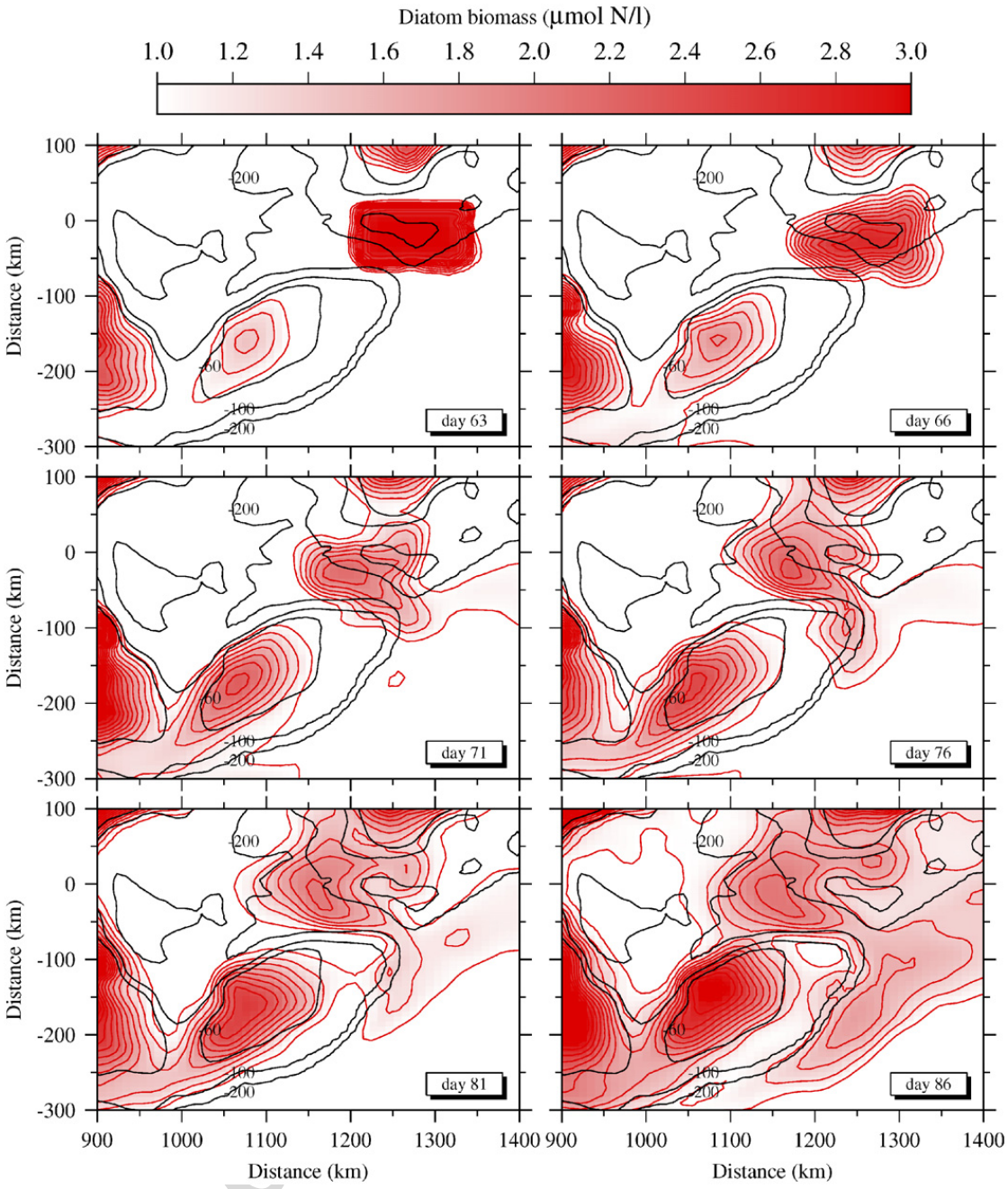

Fig. 19. Selected snapshots of coupled biological-physical model experiment results. The large phytoplankton at the surface layer (< 30 m) near Browns Bank was set to 3 μmol/l on day 63.

Shelf, and can affect food availability. If a mismatch of the spring phytoplankton bloom and timing of zooplankton reproduction occurs, either blooming too early or too late, the recruitment of zooplankton population might be negatively impacted. For example, if the post-bloom SSW cross-over to the southern flank occurs during March, it usually brings only nutrient-depleted surface water. During April, the water from the GOM could also be nutrient depleted, since the development of the spring bloom in the GOM usually occurs at this time (as a result of the stratification induced by the increased surface heat flux). A continuous lack of nutrient supply is most likely the cause of zooplankton food limitation on the southern flank of the bank during this time of the year. On the other hand, if the spring phytoplankton bloom occurs too early in comparison with the *C. finmarchicus* cohort development, much of the phytoplankton will not be grazed and therefore settle to the bottom and

enter benthic food chains (Townsend and Cammen, 1988). Observations from the southern GOM during 1988 and 1989 have demonstrated these dynamics. Early bloom initiation usually corresponds with early termination of the bloom owing to the depletion of the nutrients, which may have an even more extensive impact on *C. finmarchicus*: the cohort receives less food before it goes into post-summer diapause. The animal size will be small, energy reserves low, and development retarded. Consequently, diapause survival will be reduced. On the other hand, if the spring bloom occurs too late, food limitation will be imposed on the growth and reproduction of the G1 population. As a result, recruitment of *Calanus* for this year will be less successful. Although there may be less food limitation of the later cohort, the small population size due to the early food limitation would mean fewer individuals to go into diapause and reduced recruitment for the next year.

5. Summary

The possible sources of an intense phytoplankton bloom that occurred on the southern flank of GB during March 1999 were investigated. 3-D model experiments were conducted to examine the causes of the bloom and explore the impact of SSW on bloom dynamics. FVCOM provided the hydrodynamic fields for the Lagrangian particle trajectories, tracers, and biological model experiments. The biological model consists of nine compartments: dissolved inorganic nutrients (nitrate, ammonium and silicate), phytoplankton (large and small size classes), zooplankton (large and small size classes), and detrital organic nitrogen and biogenic silica.

Surface particles released in the Browns Bank area crossed-over the NEC, reached the NEP of GB in less than 10 days, and followed the clock-wise circulation path over the southern flank of the bank. However, this experiment does not confirm that a phytoplankton bloom can cross over and reach the southern flank. Its transport appears to be limited by vertical mixing processes, which can quickly dilute the high concentration of phytoplankton as the water moving across the NEC and reach the southern flank. The results of the coupled biophysical model indicate that the maintenance of salinity-induced stratification, as well as in situ growth of phytoplankton, are essential for inducing and maintain a spring bloom over the southern flank during March 1999.

These modeling experiments suggest that the timing and location of phytoplankton blooms on the southern flank of GB are sensitive to the advection process, which might impact the spatial distribution of temperature and salinity on the bank, the intensity of vertical stratification, the flow fields across the NEC, and the location of the salinity front near the shelf break.

Acknowledgments

This research was supported by the US GLOBEC/GB IV Program through NSF Grants OCE0227679 and OCE0234545, NOAA Grant NA16OP2323, Georgia Sea Grant College Program NA06RG0029 to Changsheng Chen; a Woods Hole Oceanographic Institute Coastal Ocean Institute Postdoctoral Scholarship to Rubao Ji; NSF Grant OCE02-20111 to Peter Franks and Edward Durbin; NSF Grant OCE0227679 to Robert Beardsley; NSF Grant OCE-0236270 to Robert Houghton, David Townsend and Gregory Lough. We want to thank Qichun Xu, Geoff Cowles, Song Hu and Hedong Liu for their help with the setup of the GOM/GB hydrodynamics model. The comments of two anonymous reviewers are gratefully acknowledged. Special thanks go to Brian Binder (University of Georgia) and Cabell Davis (WHOI) for their help on the manuscripts and their continuing support. The US GLOBEC contribution number is 303, Lamont-Doherty Earth Observatory contribution number is 6932.

References

Beardsley, R.C., Butman, B., Geyer, W.R., Smith, P., 1997. Physical oceanography of the Gulf of Maine: an update. In: Proceedings of the Gulf of Maine Ecosystem Dynamics Scientific Symposium and Workshop. Regional Association for Research in the Gulf of Maine, Hanover NH, USA. pp. 39–52.

Bigelow, H.B., 1927. Physical oceanography of the Gulf of Maine. Bulletin of the United States Bureau of Fisheries 40, 511–1027.

Bisagni, J.J., Beardsley, R.C., Ruhsam, C.M., Manning, J.P., Williams, W.J., 1996. Historical and recent evidence of Scotian shelf water on southern Georges Bank. Deep Sea Research II 43, 1439–1472.

Bisagni, J.J., Smith, P.C., 1998. Eddy-induced flow of Scotian Shelf water across Northeast Channel, Gulf of Maine. Continental Shelf Research 18, 515–539.

Blumberg, A.F., 1994. A Primer of ECOM3D-Si. HydroQual, Inc., Mahwah, NJ, 84pp.

Butman, B., Loder, J.W., Beardsley, R.C., 1987. The seasonal mean circulation: observation and theory. In: Backus, R.H.,

Bourne, D.W. (Eds.), Georges Bank. MIT Press, Cambridge, MA, pp. 125–138.

Campbell, R.G., Runge, J.A., Durbin, E.G., 2001. Evidence for food limitation of *Calanus finmarchicus* production rates on the southern flank of Georges Bank during April, 1997. Deep Sea Research II 48, 531–550.

Chen, C., Beardsley, R., 1998. Tidal mixing and cross-frontal particle exchange over a finite amplitude asymmetric bank: a model study with application to Georges Bank. Journal of Marine Research 56, 1163–1201.

Chen, C., Beardsley, R., 2002. Cross-frontal water exchange on Georges Bank: modeling exploration of the US GLOBEC/ Georges Bank phase III study. Journal of Oceanography 58, 403–420.

Chen, C., Beardsley, R.C., Franks, P.J.S., 2001. A 3-D prognostic model study of the ecosystem over Georges Bank and adjacent coastal regions. Part I: physical model. Deep Sea Research II 48, 419–456.

Chen, C., Liu, H., Beardsley, R.C., 2003a. An unstructured, finite-volume, three-dimensional, primitive equation oceanography model: application to coastal oceanography and estuaries. Journal of Atmospheric and Oceanic Technology 20, 159–186.

Chen, C., Xu, Q., Beardsley, R.C., Franks, P.J.S., 2003b. Model study of the cross-frontal water exchange on Georges Bank: a three-dimensional Lagrangian experiment. Journal of Geophysical Research 108, 3142.

Chen, C., Beardsley, R., Hu, S., Xu, Q., Liu, H., 2005. Using MM5 to hindcast the ocean surface forcing fields over the Gulf of Maine and Georgs Bank region. Journal of Atmospheric and Oceanic Technology 22, 131–145.

Cloern, J.E., 1996. Phytoplankton bloom dynamics in coastal systems: a review with some general lessons from sustained investigation of San Francisco Bay, California. Reviews of Geophysics 34, 127–168.

Durbin, E.G., Garrahan, P.R., Casas, M.C., 2000. Abundance and distribution of *Calanus finmarchicus* on the Georges Bank during 1995 and 1996. ICES Journal of Marine Science 57, 1664–1685.

Flagg, C.N., 1987. Hydrographic structure and variability. In: Backus, R.H., Bourne, D.W. (Eds.), Georges Bank. MIT Press, Cambridge, MA, pp. 108–124.

Franks, P.J.S., Chen, C., 1996. Plankton production in tidal fronts: a model of Georges Bank in summer. Journal of Marine Research 54, 631–651.

Franks, P.J.S., Chen, C., 2001. A 3-D prognostic numerical model study of the Georges Bank ecosystem. Part II: biological–physical model. Deep Sea Research II 48, 457–482.

Hopkins, T.S., Garfield, N., 1981. Physical origins of Georges Bank water. Journal of Marine Research 39, 465–500.

Houghton, R.W., 2002. Diapycnal flow through a tidal front: a dye tracer study on Georges Bank. Journal of Marine Systems 37, 31–46.

Houghton, R.W., Ho, C., 2001. Diapycnal flow through the Georges Bank tidal front: a dye tracer study. Georphysical Research Letter 28, 33–36.

Ji, R., Chen, C., Franks, P.J.S., Townsend, D.W., Durbin, A.G., Beardsley, R., Lough, R.G., Houghton, R.W., 2006. Spring bloom and associated lower trophic level food web dynamics on Georges Bank: 1-D and 2-D model studies. Deep Sea Research II, this issue [doi:10.1016/j.dsr2.2006.08.008].

Lewis, C.V.W., Chen, C., Davis, C.S., 2001. Effect of winter wind variability on plankton transport over Georges Bank. Deep Sea Research II 48, 137–158.

Lucas, L.V., Koseff, J.R., Monismith, G., Cloern, J.E., Thompson, J.K., 1999. Processes governing phytoplankton blooms in estuaries. II: the role of horizontal transport. Marine Ecology Progress Series 187, 17–30.

Lynch, D.R., Gentleman, W.C., McGillicuddy, D.J., Davis, C.S., 1998. Biological/physical simulations of *Calanus finmarchicus* population dynamics in the Gulf of Maine. Marine Ecology Progress Series 169, 189–210.

Malone, T.C., Hopkins, T.S., Falkowski, P.G., Whitledge, T.E., 1983. Production and transport of phytoplankton biomass over the continental shelf of the New York, Bight. Continental Shelf Research 1, 305–337.

Marra, J., Houghton, R.W., Boardman, D.C., Neale, P.J., 1982. Variability in surface chlorophyll *a* at a shelf-break front. Journal of Marine Research 40, 575–591.

Meise, C., O'Reilly, J.E., 1996. Spatial and seasonal patterns in abundance and age-composition of *Calanus finmarchicus* in the Gulf of Maine and on Georges Bank: 1977–1987. Deep Sea Research II 43, 1473–1501.

Mellor, G.L., Yamada, T., 1982. Development of a turbulence closure model for geophysical fluid problems. Reviews of Geophysics and Space Physics 20, 851–875.

Miller, C.B., Lynch, D.R., Carlotti, F., Gentleman, W., Lewis, C.V.W., 1998. Coupling of an individual-based population dynamic model of *Calanus finmarchicus* to a circulation model for the Georges Bank region. Fisheries Oceanography 7, 219–234.

Naimie, C.E., Limeburner, R., Hannah, C.G., Beardsley, R.C., 2001. On the geographic and seasonal patterns of the near-surface circulation on Georges Bank—from real and simulated drifters. Deep Sea Research II 48, 501–518.

Nelson, D.M., McCarthy, J.J., Joyce, T.M., Ducklow, H.W., 1989. Enhanced near-surface nutrient availability and new production resulting from frictional decay of a Gulf Stream warm-core ring. Deep Sea Research I 36, 705–714.

O'Reilly, J.E., Evans-Zetlin, C.E., Busch, D.A., 1987. Primary production. In: Backus, R.H., Bourne, D.W. (Eds.), Georges Bank. MIT Press, Cambridge, MA, pp. 220–233.

Petrie, B., Yeats, P., 2000. Annual and interannual variability of nutrieents and their estimated fluxes in the Scotian Shelf—Gulf of Maine region. Canadian Journal of Fisheries and Aquatic Sciences 57, 2536–2546.

Riley, G.A., 1941. Plankton studies. IV Georges Bank. Bulletin of the Bingham Oceanographic Collection 7, 1–73.

Ryan, J.P., Yoder, J.A., Cornillon, P.C., 1999. Enhanced chlorophyll at the shelfbreak of the Mid-Atlantic Bight and Georges Bank during the spring transition. Limnology and Oceanography 44, 1–11.

Ryan, J.P., Yoder, J.A., Townsend, D.W., 2001. Influence of a Gulf stream warm-core ring on water mass and chlorophyll distributions along the southern flank of Georges Bank. Deep Sea Research II 48, 159–178.

Smith, R.C., Baker, K.S., 1985. Spatial and temporal patterns in pigment biomass in Gulf Stream warm-core ring 82B and its environs. Journal of Geophysical Research 90, 8859–8870.

Thomas, A.C., Townsend, D.W., Weatherbee, R., 2003. Satellite-measured phytoplankton variability in the Gulf of Maine. Continental Shelf Research 23, 971–989.

Townsend, D.W., Cammen, L.M., 1988. Potential importance of the timing of spring plankton blooms to benthic pelagic

coupling and recruitment of juvenile demersal fishes. Biological Oceanography 5, 215–229.

Townsend, D.W., Thomas, A.C., 2001. Winter–spring transition of phytoplankton chlorophyll and inorganic nutrients on Georges Bank. Deep Sea Research II 48, 199–214.

Townsend, D.W., Thomas, M., 2002. Springtime nutrient and phytoplankton dynamics on Georges Bank. Marine Ecology Progress Series 228, 57–74.

Yentsch, C.S., Phinney, D.A., 1985. Rotary motions and convection as a means of regulating primary production in warm core rings. Journal of Geophysical Research 90, 3237–3284.